

RELATIVE AND ABSOLUTE YIELDS
IN THE THERMAL NEUTRON FISSION
OF U^{233}

RELATIVE AND ABSOLUTE
YIELDS
IN THE THERMAL NEUTRON FISSION OF U²³³

by
DONALD EDWARD IRISH, B.Sc.

A Thesis
Submitted to the Faculty of Science
in Partial Fulfilment of the Requirements
for the Degree
Master of Science

McMaster University

September, 1956

MASTER OF SCIENCE (1956)
(Physics)

McMASTER UNIVERSITY
Hamilton, Ontario

TITLE: Relative and Absolute Yields in the Thermal Neutron Fission
of U²³³.

AUTHOR: Donald Edward Irish, B.Sc. (University of Western Ontario).

SUPERVISOR: Richard H. Tomlinson, Ph.D.

NUMBER OF PAGES: vii, 76.

SCOPE AND CONTENTS:

A ten-inch radius, 90° sector, solid source mass spectrometer was assembled and put into operation. A description of the instrument together with the methods used to determine the fission yields resulting from the thermal neutron fission of U²³³ are reported. The mass spectrometric techniques have led to the determination of the stable and long-lived isotopes of strontium, yttrium, zirconium, cesium, neodymium and samarium. Absolute yields were obtained for the cesium and neodymium isotopes by utilizing the isotope dilution technique.

ACKNOWLEDGEMENTS

It is a pleasure to acknowledge the generous advice, encouragement and assistance of Dr. R. H. Tomlinson throughout the course of this investigation. The author is also thankful to Dr. W. Fleming, Mr. T. J. Kennett and Dr. C. C. McMullen for many helpful discussions and to his fellow group members for their co-operation.

The author is indebted to the Ontario Research Foundation for a Scholarship awarded him during the past academic year, and to Atomic Energy of Canada Limited for the service provided concerning the preparation and irradiation of samples.

TABLE OF CONTENTS

	<u>Page</u>
GENERAL INTRODUCTION	1
HISTORICAL INTRODUCTION	6
(A) Radiochemical Analysis of U ²³³ Fission Products	6
(B) Mass Spectrometric Analysis of U ²³³ Fission Products.	8
EXPERIMENTAL	13
(A) Mass Spectrometry	13
(a) The Six-Inch Mass Spectrometer	13
(b) The Ten-Inch Mass Spectrometer	13
(c) Operation of the Mass Spectrometers	24
(i) Filament Preparation and Loading	24
(ii) Mass Discrimination	25
(B) A Study of Contamination from Quartz	25
(C) Uranium-233 and Fission Products	27
(a) Irradiation	27
(b) Flux Monitoring	29
(c) Chemical Procedures	30
(i) Treatment of Sample A	30
(ii) Treatment of Samples B and C	31
(iii) Isotope Dilution	32

	<u>Page</u>
EXPERIMENTAL RESULTS	34
(A) Mass Discrimination	34
(B) Fission Yields of Uranium-233	35
(a) Flux Monitoring	35
(b) Uranium	36
(c) Strontium	37
(d) Yttrium	38
(e) Zirconium	39
(f) Cerium	41
(g) Cesium	43
(i) Relative Yields	43
(ii) Absolute Yields	44
(h) Neodymium	45
(i) Relative Yields	45
(ii) Absolute Yields	45
(i) Samarium	48
DISCUSSION	50
BIBLIOGRAPHY	61
APPENDIX	67

LIST OF ILLUSTRATIONS

	<u>Page</u>
Figure 1. Schematic Diagram of 10-inch Mass Spectrometer Tube ..	14
Figure 2. Multiple Filament Surface Ionization Source	15
Figure 3. Source End of Mass Spectrometer Tube	18
Figure 4. Allen Type Multiplier	20
Figure 5. Collector Assembly - Internal Details	21
Figure 6. Complete Collector Assembly	22
Figure 7. Typical Mass Spectrogram of Neodymium	47
Figure 8. Light Mass Distribution from U ²³³ Fission	53
Figure 9. Heavy Mass Distribution from U ²³³ Fission	60
Figure 10. Comparison of Light and Heavy Mass Yields in Thermal Neutron Fission of U ²³³	62

LIST OF TABLES

<u>Table</u>		<u>Page</u>
I	Irradiation Data for Uranium Samples	27
II	Isotope Dilution Solutions	32
III	Isotope Dilution of Samples B and C	33
IV	Cesium Ratios as Observed on Various Collectors	34
V	Neodymium Ratios as Observed on Various Collectors	35
VI	Flux Determinations with Cobalt Monitors	36
VII	Relative Abundances of Uranium in Samples B and C	37
VIII	Relative Fission Yields of Strontium Isotopes	38
IX	Relative Fission Yields of Yttrium Isotopes	39
X	Relative Fission Yields of Zirconium Isotopes in Sample B	40
XI	Relative Abundances of Cerium in U ²³³ Fission (Isotope Diluted Sample C).....	42
XII	Relative Fission Yields of Cesium Isotopes	43
XIII	Isotope Dilution Data for Cesium	44
XIV	Relative Fission Yields of Neodymium Isotopes	46
XV	Isotope Dilution Data for Neodymium in Sample C	48
XVI	Relative Abundances of Samarium Isotopes in U ²³³ Fission (Sample B)	49
XVII	Fission Yields of Light Fragments Formed in the Thermal Neutron Fission of U ²³³	51
XVIII	Absolute Fission Yields of Heavy Fragments Formed in the Thermal Neutron Fission of U ²³³	56

GENERAL INTRODUCTION

Shortly after the discovery of the neutron in 1932 Enrico Fermi (1) and his collaborators in Italy began neutron irradiation of many elements, including uranium. In this latter case artificial activities were observed and credited to transuranium elements produced as a result of neutron capture. This phenomenon aroused the interest of other workers. In France, Curie and Savitch (2) chemically separated a 3.5-hour activity from irradiated uranium and the German scientists, Hahn and Strassmann (3), proved that this must be assigned to an isotope of barium. The detection, in 1939, of yet other nuclides led Meitner and Frisch (4) to conclude that the uranium nucleus, after neutron capture, divides itself into two nuclei of roughly equal size. They borrowed the word "fission" from the biologists to describe this splitting. A radically new nuclear reaction had been discovered.

Since that time fission has been induced both by particles and electromagnetic radiation in many nuclei with mass greater than 200. The first observed fission reaction, however, thermal* neutron fission, is still of the greatest practical and theoretical importance.

The tremendous release of energy accompanying the fission reaction was first utilized during wartime in the atomic bomb. In a

* The term "thermal" applies to neutrons with 0.025 ev. energy

now peaceful world, fission, controlled in nuclear reactors, is used for production of power, synthesis of isotopes and fundamental research. Three readily available isotopes, viz. U^{235} , U^{233} and Pu^{239} , are capable of undergoing thermal neutron fission. Although U^{235} is only 0.719% abundant in natural uranium it is possible, in a reactor operating on the basis of U^{235} fission, to breed the two other fissionable materials U^{233} and Pu^{239} from the comparatively abundant Th^{232} and U^{238} . The world's supply of material, capable of undergoing thermal neutron fission, is therefore greatly enhanced.

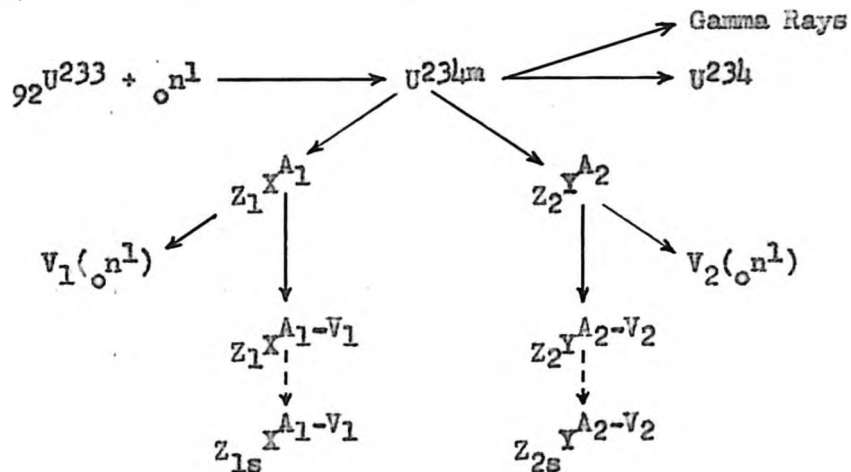
U^{233} is synthetically derived from natural thorium in the following manner. When Th^{232} absorbs a neutron it becomes the short-lived isotope Th^{233} (half-life: 23 minutes). This emits a beta particle and is transmuted to Pa^{233} (half-life: 27 days) which in turn loses another beta particle and becomes U^{233} . This thesis is concerned with the determination of the quantities of materials, called fission products, produced from the fission of the U^{233} .

When U^{233} absorbs a thermal neutron a metastable compound nucleus, U^{234m} , is formed. This nucleus may de-excite by emission of gamma rays to produce the alpha active U^{234} ; or it may divide into two primary fission fragments. Symmetrical fission ($A \sim 116$) is rare; it happens in only about 0.01% of the instances. The most common occurrence is a splitting into two fragments with mass numbers approximately 93 and 139. The primary fragments are unstable because their neutron to proton ratio is too large for stability. Hence prompt neutrons (2.59/fission for U^{233}) (5) are emitted from the primary fragments within 10^{-13} seconds. Delayed neutrons, amounting

to 1% of the total, are emitted with half-lives of the order of seconds.

The primary fission fragments decay by beta emission thus decreasing the neutron to proton ratio of the nuclei and increasing their stability. About 66 such fission product chains have been observed averaging three members each.

The U^{233} fission process is summarized by the following equation:



where $Z_1 X^{A_1}$ and $Z_2 Y^{A_2}$ are primary fission fragments of light and heavy mass respectively,

V_1 and V_2 are the numbers of neutrons emitted,
 $Z_1 X^{A_1-V_1}$ and $Z_2 Y^{A_2-V_2}$ are the fission products undergoing beta decay,

$Z_{1s} X^{A_1-V_1}$ and $Z_{2s} Y^{A_2-V_2}$ are the stable fission products.

A large amount of energy is released in the fission process and subsequent events. For U^{233} (6) the most probable kinetic

energy of the light fragment is 99.1 Mev; of the heavy fragment 63.9 Mev. The prompt neutrons and prompt gamma rays possess 5 Mev. each and the beta and gamma decay of the fission products dissipate 11 Mev. This represents a total of 184 Mev. of energy, which, in the presence of an absorber such as the moderator of a reactor, appears in the form of heat.

The primary fission yield of a nuclide may be defined as the percentage of fissions which result in the formation of that nuclide. A cumulative fission yield is the sum of all primary fission yields of a given mass,

i.e. cumulative yield of mass A (%) =

$$\frac{\text{sum of the number of fission atoms of mass A} \times 100}{\text{number of fissions}}$$

The number of atoms formed may be determined by either radiochemistry or by mass spectrometry utilizing the isotope dilution technique. The latter method has proven its superiority and to a great extent has superseded the former.

The number of fissions has been determined in several ways. The most direct methods involve either measurement of the loss of weight of uranium during the irradiation (7) or counting of the number of fissions with a pulse ionization chamber (3). Indirect methods involve measuring the extent of neutron absorption by some other nuclide such as B^{10} (9) (10) whose probability of interaction with neutrons relative to uranium is known.

This thesis constitutes a report of the measurement of the fission yields of some of the fission fragments produced by thermal

neutron irradiation of U^{233} . The method utilizes isotope dilution and mass spectrometry to determine the number of fission atoms of a given mass and Co^{59} monitoring to determine the number of fissions. The absolute cumulative fission yields of masses 133, 135, 137, 142, 143, 144, 145, 146, 148 and 150 constituting part of the heavy mass distribution have been determined. The relative yields of masses 88, 89, 90, 91, 92, 93, 94 and 96 of the light mass distribution and masses 147, 149, 151 and 152 of the heavy mass distribution are also reported. A ten-inch radius, 90° sector, solid source mass spectrometer was assembled to obtain these data. Details concerning its construction and performance are also included.

These results are of importance to efficient nuclear reactor design and operation. In particular the abundance of nuclides emitting delayed neutrons or having high neutron capture cross sections (reactor "poisons") are of prime concern in reactor operation. A knowledge of the distribution of radioactivities is important for such problems as shielding requirements, decontamination and waste disposal. The results also augment the accumulation of knowledge already assembled on fission yields which stand as a final body of facts to be explained by any quantitative theory of fission.

HISTORICAL INTRODUCTION

A. Radiochemical Analysis of U²³³ Fission Products

The isotope U²³³ was first separated and examined in 1942 by Seaborg, Gofman and Stoughton (11). These workers showed that the isotope undergoes fission with thermal neutrons. From 1944-46 Seaborg and collaborators (12) studied the chain of decay products from this new isotope. The decay products constituted a substantial fraction of the $4n + 1$ radioactive series, called the neptunium series after the longest lived member. U²³³ was found to be an alpha emitter with half-life of 1.63×10^5 years, which, after six alpha emissions and three beta emissions, decays to the stable Bi²⁰⁹. Independent work carried out by English et al (13) substantiated this evidence.

In 1948 Grummitt and Wilkinson (14) reported the first U²³³ fission yields, consisting of 19 nuclides between masses 89 and 147. Stable isotopic carrier was added for each nuclide and then each element was separated chemically from the rest. The resulting activities were measured by means of counting techniques. The yields were obtained by relating the activities to that of Ba¹⁴⁰, whose fission yield was arbitrarily assigned the value 6.7%. At best these results were only considered reliable to 10-20%. A mass-yield plot showed that the double humped curve, indicating a light mass group and a heavy mass group, had maxima which were displaced one unit lower on the mass scale than the similar curve for U²³⁵ fission.

In the same year an independent determination of the fission yields published by Steinberg (15) was declassified. The number of fissions occurring in the sample was determined by direct count in a pulse ionization chamber. In order to minimize self-absorption of fission recoils and resolution losses at high counting rates, only a small sample could be used in the fission counter. A larger sample, which was to be used for fission product analyses, was placed just outside the fission chamber so as to be irradiated with the same neutron flux as the light sample. The number of fissions occurring in the larger sample was calculated from the number counted in the light sample and the ratio of sample weights. The heavy sample was dissolved and radiochemically analyzed for the fission products of interest.

By this means the absolute fission yields of Ba¹⁴⁰ and Mo⁹⁹ were found to be 6.0% and 4.7% respectively, with a quoted accuracy of 15%. These were used as monitors in assigning the absolute yields to 16 other nuclides, which were determined relatively, but for which the fissions had not been directly counted. Nuclides with half-lives of the order of days and which decay by emission of a single beta particle were chosen.

The results of this work were significantly different from the earlier work of Grummitt and Wilkinson (14). The light mass distribution was observed to shift two mass units lower in relation to the equivalent distribution for U²³⁵, a result substantiated by the ionization chamber studies of Deutsch and Ramsey (16).

A radiochemical analysis of 36-second I^{136} appearing in U^{233} fission was reported by Stanley and Katcoff (17) in 1949. The yield was normalized to Ba^{139} , which was interpolated from the data of Steinberg et al (15). The yield $1.7 \pm 0.3\%$ was obtained.

The results of the foregoing radiochemical analyses assigned a smooth yield-mass curve to U^{233} , similar to those first reported for U^{235} and Pu^{239} , (18). The latter two, however, were later found to have fine structure when more accurate work was carried out (6).

B. Mass Spectrometric Analysis of U^{233} Fission Products

The mass spectrometer was first applied to the study of isotopes resulting from fission by Thode and Graham (19). Their investigation of the gases xenon and krypton, resulting from the thermal fission of U^{235} , indicated results which could not be reconciled with a smooth mass-yield curve. Further work by Macnamara, Collins and Thode (20) indicated that Xe^{134} was formed in a yield about 30% higher, and Xe^{133} about 20% higher, than that predicted from former studies. For the first time fine structure had been observed in the fission yield distribution.

From this work it was seen that the mass spectrometer was particularly suited to the study of fission products. It was the only method that gave information about the stable end products of the fission product decay chains. It permitted the positive identification of mass numbers and relative fission yield data. Since the mass spectrometer only measures the ratios of the isotopes of an element, losses during chemical separations and manipulations do not influence the relative yields obtained, providing there is no

isotopic fractionation.

At first only relative yields of the isotopes of an element were obtained and these were put on an absolute basis by assuming the best value obtained by radiochemical means for one of the mass chains, e.g. relative yields of the mass chains 131, 132, 134 and 136 obtained from the mass spectrometric ratios of the Xe isotopes were given absolute values by normalizing to the yield of the 131 mass chain obtained from the radiochemical determination of ^{131}I (21). With the advent of the isotope dilution technique it became possible to obtain fission product analyses completely independent of counting experiments. As excellent reviews (22) (23) of this method are available, only brief mention of it will be made here.

A weighed portion of the sample to be analyzed for a certain element is diluted with a weighed aliquot of a standard stock solution having different isotopic composition than the elements under investigation. The mixture is processed through appropriate steps to ensure that the components achieve equilibrium. The isotopic composition of each element is then obtained with the mass spectrometer and related to the isotopic composition of an undiluted portion. Naturally-occurring elements may be used for the isotope dilution of fission products because their isotopic composition is very different. In fact, a natural isotope may actually be missing; or radioactive isotopes with half-lives long enough for mass spectrometric analyses may be present in the fission products. The absolute yields can be determined under any of these circumstances by solving a suitable set of simultaneous equations.

The experimental work in this thesis illustrates the procedure. The method is limited to elements which have more than one measurable isotope. Errors are attributable to contamination and sample inhomogeneity. These factors may limit the accuracy of particular results but not the limit of the method.

Mass spectrometric fission yields of U^{233} were first obtained by Steinberg et al (24) in 1954. Relative isotopic abundances of fission-produced zirconium, molybdenum and ruthenium indicated that fine structure having a maximum at mass 99 existed in the light mass group, similar to that reported in U^{235} (25).

Further work was carried on by Fleming, Tomlinson and Thode (26) in an attempt to ascertain and compare the fine structure, particularly on the heavy mass distribution of U^{233} fission products with the fine structure already known for U^{235} . They measured the stable and long-lived isotopes of xenon, cesium and krypton. The Xe yields were normalized by assuming a yield for I^{132} of 4.9% (14). The data showed no evidence of fine structure, although in the comparable portion of the U^{235} fission yield curve abnormally high yields occur at masses 133 and 134. Two mechanisms had been advanced to explain this. Glendenin (27) suggested that the loosely held 83rd neutron was emitted by the highly excited, primary fission product. Alternately Wiles et al (21) suggested that nuclei with 82 neutrons may be favored in the primary fission process.

Pappas (28) extended the Glendenin hypothesis to include preferential neutron emission of the 85th, 87th and 89th neutrons from primary fission fragments. These ideas have been combined to give a

quantitative prediction of the U^{235} fission yields. Pappas has predicted abnormally high yields at masses 132 and 133 in U^{233} fission and at 134 and 135 in U^{233} fission. Experimental data agreed with the former prediction but the yields from U^{233} gave no confirmation to the latter supposition. The discrepancy between theory and experiment was not explained but was thought to be the result of either charge division or mass difference.

In 1955 two papers appeared in the literature concerning U^{233} fission. The first of these (29) was a report on the relative abundances of neodymium and samarium isotopes in the thermal neutron fission of U^{233} . A sample of uranium containing 14.4 atom % U^{233} , 0.6 atom % U^{235} and 85.0 atom % U^{238} was irradiated. The relative ratios were obtained from this sample mass spectrometrically. Corrections were applied for contamination, cerium hold up at mass 144, neutron capture at mass 149 and contribution to the fission products from 0.6 atom % U^{235} present. The results in this mass region were compared with U^{235} fission yields and it was shown that the U^{233} yields decrease more rapidly with increase of mass of the fission product.

The second paper (7) was presented at the July Conference of the Academy of Sciences of the U.S.S.R. on the Peaceful Uses of Atomic Energy. This paper reports the absolute fission yields obtained from the isotope dilution and mass spectrometric analysis of neodymium and cerium. The U^{233} underwent a lengthy irradiation in a nuclear reactor and the number of fissions were determined from the loss of weight in the uranium.

The relative yields of Nd isotopes agree with those reported by Melaika et al (29) except at mass 144, which the Russians found to be much lower. The absolute yield at mass 140 was reported as 5.6% compared to 6% given by Steinberg (15).

Two surveys of fission yields have recently been compiled. The first of these was presented by Steinberg and Glendenin at the Geneva Conference (25). This includes a review of the current theories used to interpret the detailed features of the mass yield distribution. The best data from all possible sources have been compiled by Katcoff (6), who quotes yields for U^{233} fission taken from the references mentioned above (7) (24) (25) (26) (27). The yields are normalized to the yield for Ba^{140} , determined by Steinberg (15), in such a manner as to make the total yield 100% for each of the light and heavy fission product distributions.

Accuracy in measuring fission yields is still difficult to obtain, in spite of present α counting and mass spectrometric techniques. The need for more data is still great if the theory of fission and the explanation for fine structure is to be derived.

EXPERIMENTAL

A. Mass Spectrometry

(a) The Six-Inch Mass Spectrometer

A six-inch radius, 90° sector, mass spectrometer (30), with magnetic scanning and hot filament source, was used to obtain some of the results. This instrument was equipped with a vibrating reed d.c. amplifier (Model 308, Applied Physics Corporation) and a Brown Electronics recorder with a half-second response (Minneapolis-Honeywell Reg. Co.).

(b) The Ten-Inch Mass Spectrometer

A ten-inch mass spectrometer of more recent design was constructed in the instrument shops of this University and put into operation by the author. As no complete description of the instrument exists in the literature, its design and operation are discussed here.

This mass spectrometer is a ten-inch radius, 90° sector instrument, with magnetic scanning and a hot filament source. The 90° mass spectrometer tube (Fig. 1) is a vacuum tight, non magnetic, inconel envelope, consisting of the ion source system (A-Fig.1), the curved analyser tube (B-Fig.1), and an ion collector assembly (C-Fig.1).

The source (Fig. 2) is essentially the multiple filament surface ionization source, designed by Inghram (31), with the beam centering plate omitted. The filament holder assembly (F-Fig.1), which supports a central ionization filament (M-Fig.1) and two sample

FIGURE 1 : SCHEMATIC DIAGRAM OF 10" MASS SPECTROMETER TUBE

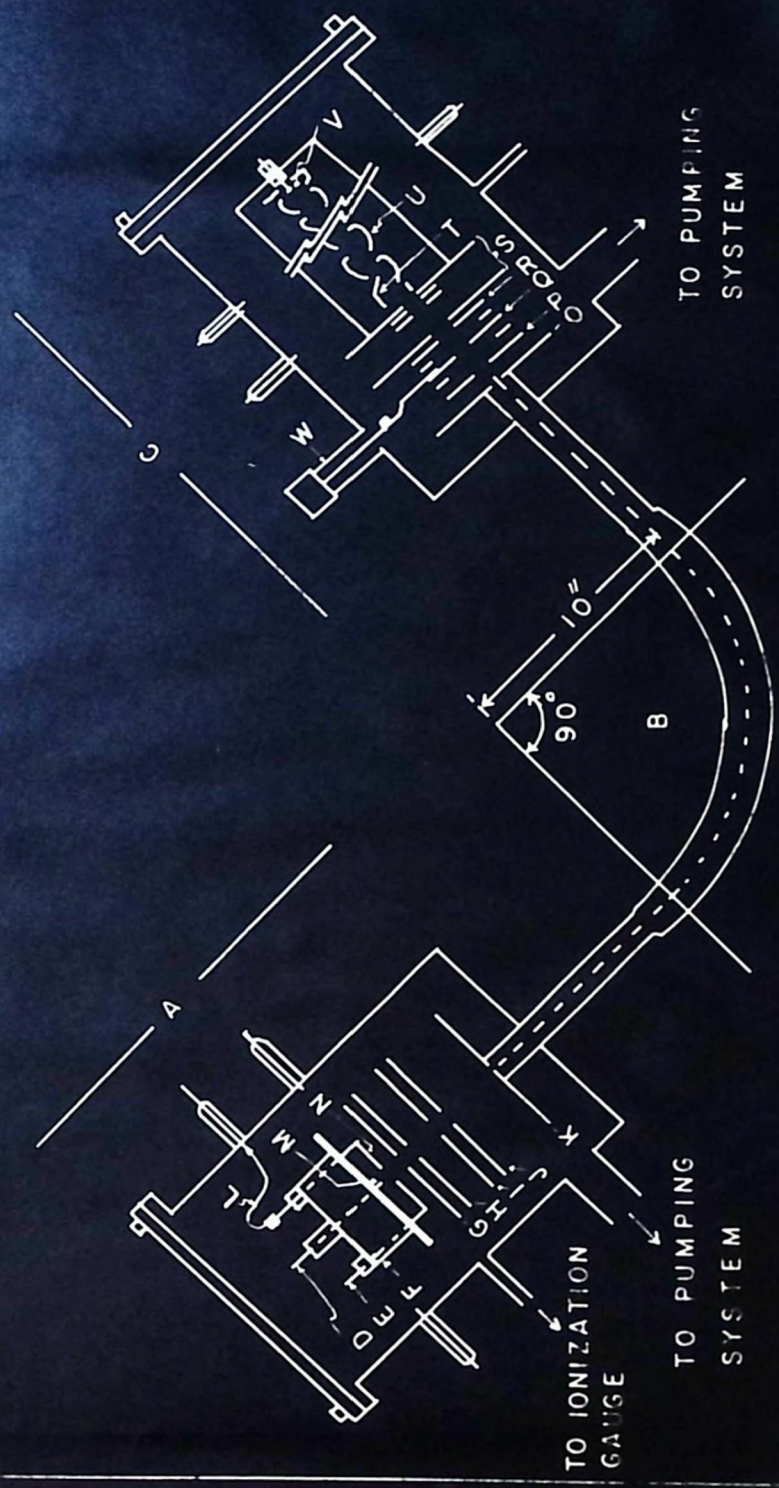


FIGURE 2Multiple Filament Surface Ionization Source

filaments (N-Fig.1), is connected to the source proper but may be removed for loading. The sample is evaporated at an appropriate temperature on to the much hotter central ionization filament where ions are formed. This permits the evaporation rate and centre filament temperature to be varied independently, improving the ionization efficiency of substances which evaporate at low temperatures. The background caused by surface ionization of hydrocarbons is another problem which is eliminated by this design. Alternatively, the mass spectrometer may be operated when samples are placed directly on the central ionization filament. This is particularly suitable for analysis of elements which give ions at temperatures below that at which they evaporate at significant rates. Insulation of the filaments from the head assembly is accomplished by standard 0.040-inch untinned Kovar-glass feedthroughs (D and E - Fig. 1). The filament and surrounding case are operated at almost the same potential, viz. 3100 volts - the most positive potential in the source.

The source plates are made of 0.020-inch Nichrome V. The first two plates after the filament, named defocussing (G-Fig.1) and discriminating (H-Fig.1) respectively, defocus the ion beam. By this means ions produced on the sample filaments may be defocused from the beam without affecting ions coming from the ionization filament. On the other hand, by suitable choice of voltages, both beams may be focused and observed. The ions are accelerated by the difference in potential between the filament and plates (J and K - Fig. 1) which are grounded. A variable potential between the pair of half-plates (I-Fig.1) permit deflection of the ion beam so that a maximum ion

intensity may be focused on the grounded collimating slits (J and K - Fig. 1).

The plates are spaced and insulated by quartz tubing. Electrical connections from the external circuitry are made through Kovar-glass feedthroughs, welded to the tube proper (Fig. 3).

Platinum wire leads (L-Fig.1), fitted with 0.040-inch nickel sleeves which slide over the Kovar rods complete the circuit to the individual plates. The voltages on the plates are supplied through a potential divider by a positive high voltage supply with output of 10,000 volts, stable to 1 part in 50,000.

The filament supply produces a continuous direct current from 0 to 8 amperes with a stability of 1 part in 30,000. Below 2.5 amperes, the current was fed through a 2 ohm resistance. This permitted the application of a sufficiently high voltage to the 2AS15 temperature sensitive diode to enable it to control the current.

An ion beam, which emerges from the final collimating slit of the source, travels in a straight line and enters the homogeneous magnetic field perpendicular to the faces of the Armco iron pole pieces. It is then deflected through an angle of 90° and leaves the field boundary perpendicularly. The magnet supply produces 300 ma maximum current at 1000 volts output. Continuous magnetic scanning is permitted by means of a motor-driven helipot which varies the current to the magnet coils.

The ion detector assembly is arranged so that the current may be detected either directly or with an electron multiplier, similar

FIGURE 3Source End of Mass Spectrometer Tube

to that used by Inghram (32). The ion beam first passes through a defining slit (O-Fig.1) and an electron repeller slit (P-Fig.1). The latter suppresses the secondary electrons, formed when the ion beam strikes a surface. The ions may be collected directly on a closed adjustable slit (Q-Fig.1), made to function by the pressure exerted on a bellows (W-Fig.1) by a micrometer screw. The voltage drop across a suitable grid leak resistance connected to this closed slit is measured by an Applied Physics Corporation vibrating reed electrometer. The output is fed to a Leeds and Northrup Speedomax recorder, so that a permanent record is obtained.

In order to use the electron multiplier collection, the adjustable slit is opened and the ions pass through a beam deflecting slit (R-Fig.1) and into an ion accelerator region composed of four slits (S-Fig.1) with a voltage drop between them, before finally striking the conversion dynode (T-Fig.1) of the Allen type multiplier (33) (Fig. 4). The collector assembly, including plates O to S, is well represented in Figures 5 and 6. The dynodes (U-Fig.1) are formed from 2 percent beryllium-copper sheet, and are mounted between lavite rods which afford insulation. The dynodes were activated in order to obtain maximum gain. This was achieved by cleaning with dilute nitric acid, washing in water and heating in an oven, through which a continuous stream of hydrogen was flowing, for 30 minutes at 625°C (34). The voltage divider network, consisting of a series of one megohm resistors enclosed in glass, is located directly on the multiplier inside the tube housing. The negative high voltage supply is similar to that used for the source.

FIGURE 4
Allen Type Multiplier

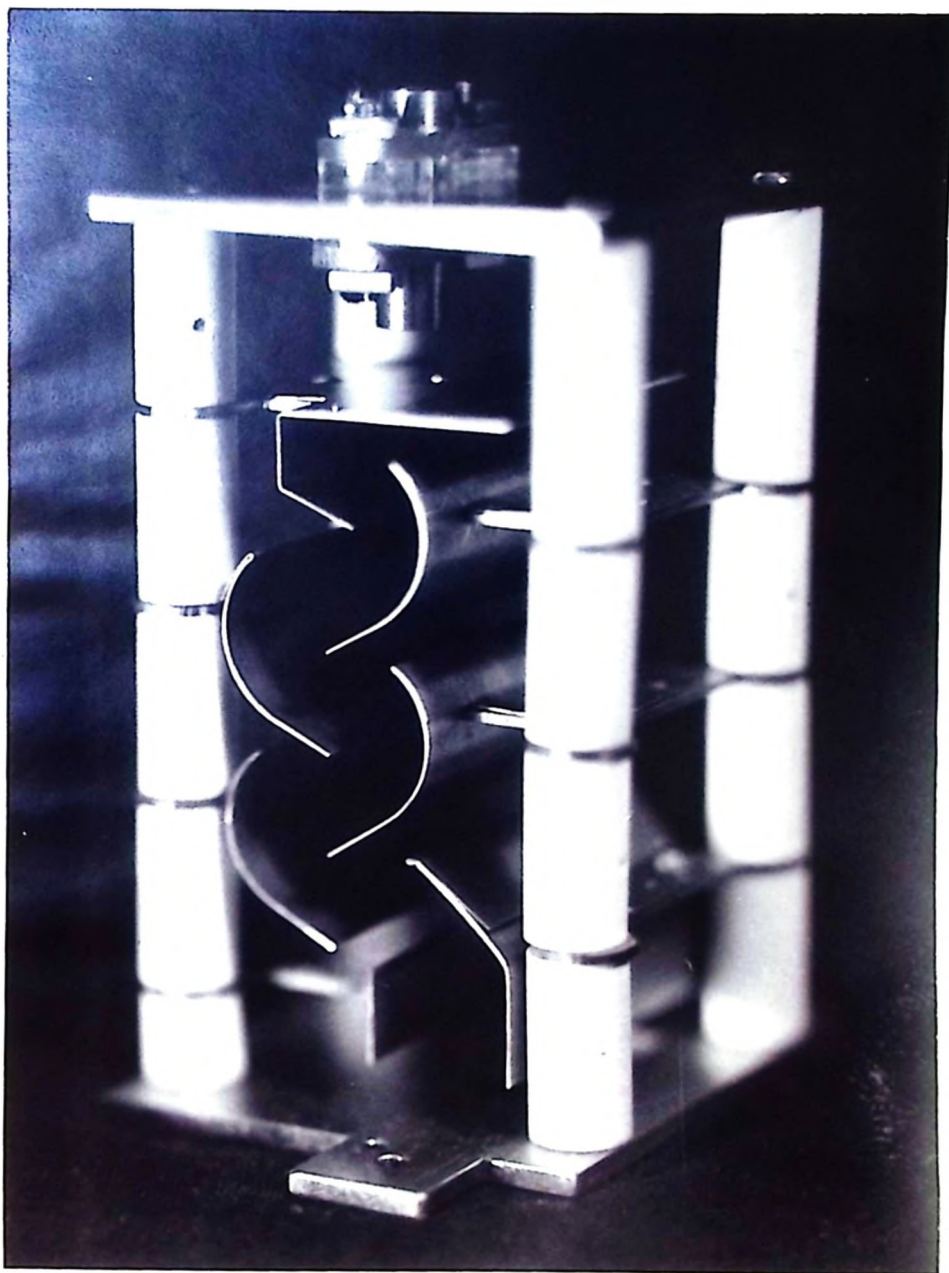
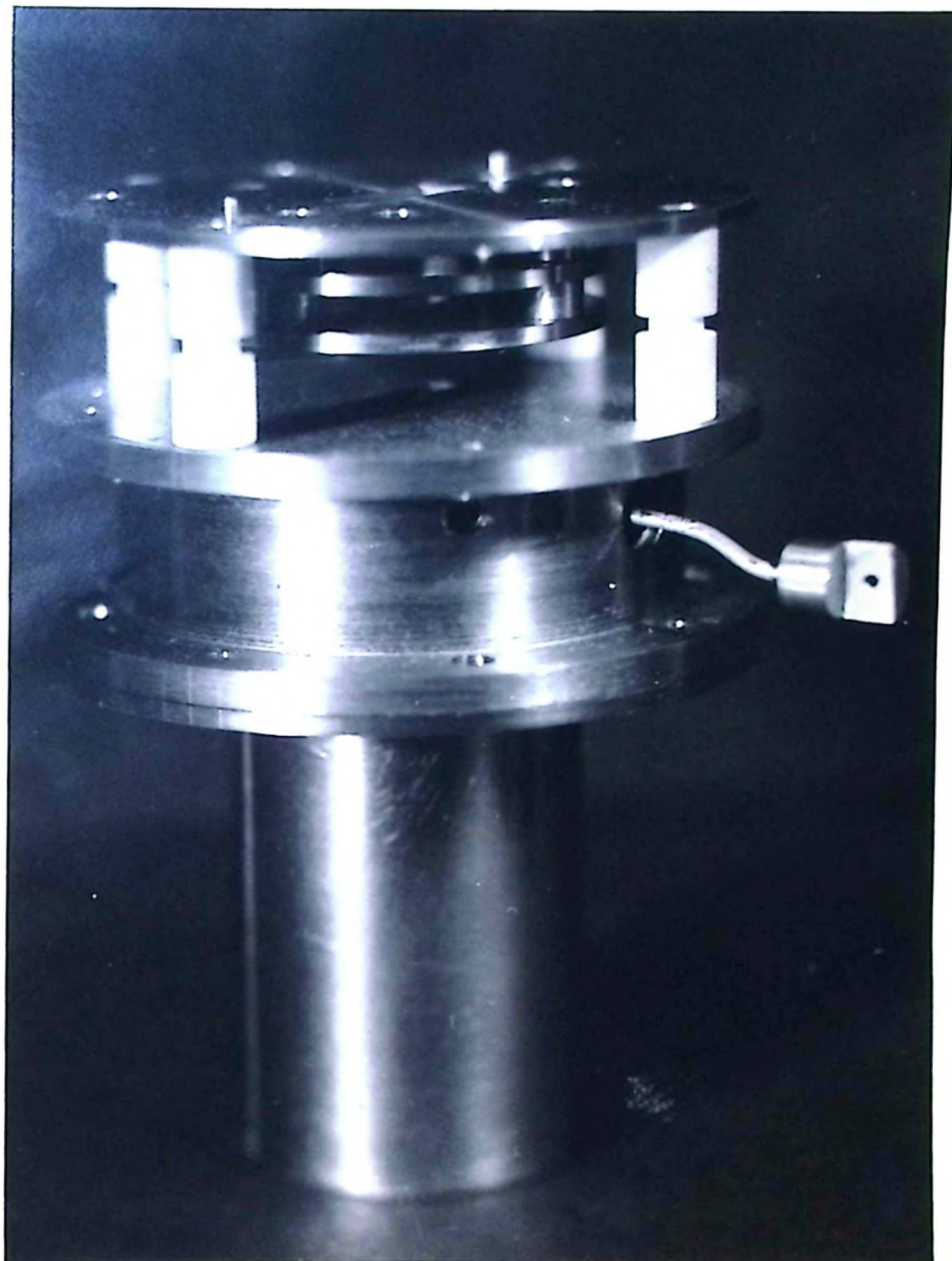


FIGURE 5Collector Assembly - Internal Details

FIGURE 6Complete Collector Assembly

The ions, which strike the conversion dynode, eject secondary electrons which are accelerated and focused on the next dynode. This process is repeated through ten identical stages, until finally the amplified electron beam is collected on an inconel plate (V-Fig.1). The current from this plate is measured and recorded in the same manner as described above for direct collection. The gain of the multiplier, as determined by direct comparison of current measurements obtained both with and without it, was found to be 5000.

The secondary electrons are capable of ionizing residual gas, if the pressure in the collector region is large. The voltage gradient tends to attract the positive ions back toward the source. These may strike active surfaces, thus producing secondary electrons, which could cause the multiplier to go into continuous discharge. In order to prevent this, the collector end of the tube was evacuated directly. A pressure of 10^{-7} mm. of mercury was maintained by means of three-stage glass mercury diffusion pumps, backed by Welch Duo-Seal fore pumps, situated at both source and collector ends. Liquid-air traps situated between the diffusion pumps and mass spectrometer tube, condense mercury and other condensible gases. Liquid-air thimbles situated above these traps could be used during actual measurements to accelerate removal of residual vapours. The tube and glass leads, wrapped with asbestos and resistance wire, were baked to remove occluded gases and materials with low vapour pressure.

The final collimating slit in the source and the initial slit in the collector are 0.3 mm. and 0.5 mm. respectively. For a ten-inch mass spectrometer a theoretical resolving power of one mass unit

in 316, determined from slit width only, is obtainable. Resolving power may also be obtained from the relation:

$$\text{Resolving Power} = \frac{\text{peak width}}{\text{peak separation} \times \text{mass number}} .$$

By proper positioning of the magnet and suitable application of voltages a resolving power of about one mass unit in 280, calculated from this formula, was obtained.

(c) Operation of the Mass Spectrometers

(i) Filament Preparation and Loading

A new filament was prepared for each mass spectrometric analysis. The central ionization filament was the only one of the three source filaments used in the present work. This filament was made of 0.001-inch x 0.030-inch tungsten, fitted to the Kovars by 0.040-inch nickel sleeves. The tungsten was platinum coated, giving it a higher work function and hence improving its ionization efficiency (35). It was electrically heated in vacuum both before and after the plating in order to free it of all volatile impurities. When positioned in the filament holder, the filament was 5 mm. from the defocussing slit. The preparation of the filament for the six-inch mass spectrometer was essentially the same, differing only in the construction of the filament holder. A drop of the solution containing the material to be analyzed was placed on the surface of the filament and evaporated to dryness.

(ii) Mass Discrimination

Mass discrimination is a commonly observed phenomenon in instruments employing electron multipliers as detectors (32). Because of their greater sensitivity, the ions are detected at much lower filament temperatures and isotope fractionation at the source may also become appreciable. As multipliers are nonlinear with mass, energy and stray magnetic fields, they should never be used unless absolutely necessary for sensitivity. Relationships concerning these effects are reported by Ingraham (32).

To determine the importance of mass discrimination, Cs and Nd ratios were obtained, both by collecting on the closed slit and on the multiplier. These ratios were compared with ratios obtained with the six-inch mass spectrometer, which was not equipped with a multiplier.

Since the results indicated no systematic variation and were consistent with their standard deviations, it was concluded that any mass discrimination was less than 1% and would cause no significant change in the data. (Conclusions are based on the data appearing in Tables IV and V). This, however, does not preclude the possibility of significant discrimination occurring with isotopes of other elements.

B. A Study of Contamination from Quartz

Uranium samples were irradiated in sealed quartz vials. During the fission process the fragments are formed with such energy that a fraction of them penetrate into the walls of the quartz vial.

For absolute yield determinations these must also be included in the analysis, in order to avoid deficiencies as well as to eliminate the possibility of fractionation. Hence it is both desirable and convenient to be able to dissolve the entire quartz vial with the uranium. In order to ascertain to what extent the fission products of interest would be contaminated by natural elements in the quartz, the following analysis was carried out.

A representative sample of quartz was crushed in a mortar and a weight equivalent to that of a vial (0.3951 gm.) dissolved in 8.5 gm. hydrofluoric acid (Baker and Adamson, 48% Reagent). 0.9709 gm. of a U^{235} stock fission product solution of known isotopic composition was then added and the mixture evaporated to dryness. It was next taken up in a drop of water, a portion was placed on the filament of the 6-inch mass spectrometer and the various spectra observed.

The measured ratio of masses 133:137, after correction for decay of the 137, was found to be 1.145. Melaika (22) had determined this ratio to be 1.167 for the same sample. Contamination from quartz would increase the amount of Cs^{133} present, as it is the only isotope of cesium in nature. Hence, if the sample were contaminated, the ratio would have been greater than the value determined by Melaika, and it is concluded therefore that no significant contamination was present.

Also, no Nd^{142} was observed and, since this is the most abundant isotope of natural neodymium, it may be concluded that neodymium contamination is also insignificant.

On the other hand, the ratio of Rb^{85}/Rb^{87} was 0.577, which is greater than the reported value 0.466. Rubidium contamination was, therefore, introduced by the quartz. Traces of strontium and cerium contamination were also observed but the extent of contamination was sufficiently small that corrections could be made to the observed mass spectrometric ratios. The methods of making corrections for contamination of the fission product elements are discussed with each table of experimental results.

G. Uranium-233 and Fission Products

Three samples of uranium oxide (A, B and C) were irradiated with thermal neutrons in the Chalk River reactor. Sample A had been allowed to "cool" for four years. Only the relative fission yields of the cesium isotopes were determined from this sample. Samples B and C were allowed to "cool" for only three months and the details concerning irradiation, flux monitoring and chemical techniques are given below.

(a) Irradiation

The irradiation data are given in Table I.

TABLE I

Irradiation Data for Uranium Samples

Sample	Weight (grams)	Proportion U^{233} in Sample (%)	Irradiation Time (days)
A	0.05	14.6	49.05
B	0.0898	6.66 *	46.59
C	0.0830	6.66 *	46.59

* Diluted with U^{238} depleted in U^{235} .

Sample A was only useful for the determination of relative fission yields as the exact weight was unknown and the flux was only approximately known from pile data. In particular, it was used for the mass spectrometric analysis of the relative fission yields of the cesium isotopes.

Samples B and C were prepared and irradiated for the express purpose of determining the absolute fission yields of cesium and neodymium. In order to make the self shielding correction small it was desirable to uniformly dilute the U^{233} with some material with low cross section for thermal neutrons. U^{238} , depleted in U^{235} , supplied by Los Alamos, was selected as the dilutant. The self shielding was further reduced by irradiating the diluted sample in a vial which approximated an infinite cylinder. The extent of the self shielding correction is calculated in Appendix D.

The U^{233} and U^{238} were converted to the oxide and combined in a ratio of approximately 1:10 by weight. This mixture was dissolved in a minimal amount of redistilled* nitric acid and hydrochloric acid. The solution was evaporated to dryness and again oxidized in a small quartz crucible over a micro burner. The resulting powder, U_3O_8 , was sealed in quartz vials about 4.4 cm long and 0.15 cm diameter. In

* All acids and peroxide used were redistilled, except hydrofluoric and perchloric acids. The distilled water was passed through a Dowex-50 ion exchange column to free it of cationic impurities. This is assumed in future discussions of chemicals.

order to monitor the flux, a weighed, 1 mil cobalt wire, wrapped in 1 S aluminum foil, was fastened around each vial. The vials were wrapped in aluminum foil and packed in an aluminum irradiation capsule. Two other flux monitors were also used in order to measure flux gradients in the region of the sample; one of these was included in the capsule and the other cold welded across the lid of the capsule. Irradiation was carried out in a "J-rod tray rod" position of the N.R.X. Chalk River Reactor.

(b) Flux Monitoring

Cobalt monitoring was selected for the following reasons: since both Co^{59} and U^{233} are $1/v$ detectors, the ratio of their cross sections is independent of neutron energies; Co^{59} has a long half-life and hence analysis can be carried out long after the irradiation; and the number of Co^{60} atoms formed by neutron absorption could be accurately determined by means of a 4π ionization chamber (Harwell Type, T.P.A. Mk II). This was a well-type instrument filled with 20 atmospheres of argon. The ion current was measured with an Applied Physics Corporation vibrating reed electrometer.

The activity of the cobalt was determined by comparing the observed ion current with that produced from a 0.150 ± 0.007 mc cobalt standard obtained from R.C. Hawkins of Chalk River. The standard source consists of a 1.0 cm length of 0.005-inch "specpure" cobalt wire weighing 1.14 mg., sealed in a length of 0.075-inch O.D. aluminum tubing. The aluminum sheath constituted approximately 0.05% of the total activity of the source, but this fraction decreased continually as it was essentially made up of 85-day Sc^{46} . The observed activity

did not require correction for decay as the cobalt standard was irradiated and standardized at the same time as Samples B and C were being irradiated. Table VI tabulates the results of the flux determinations.

(c) Chemical Procedures

(i) Treatment of Sample A

An attempt was made to dissolve the contents of vial A and etch the surface of the quartz without actually dissolving an appreciable amount of quartz. This was done by breaking the vial, soaking the contents with concentrated nitric acid, and removing the supernatant liquid. The process was repeated until the activity remaining in the quartz was about 0.5% of the total activity of the sample, as measured by an end-window Geiger tube. During the course of evaporation of the acid solution the polyethylene container degraded, contaminating the sample with organic matter and other unknown elements. As a result it was only used to obtain relative fission abundances of cesium isotopes.

The organic matter was oxidized and removed with perchloric acid. The solution was evaporated to dryness, taken up in dilute nitric acid and again evaporated to dryness. The residue was then dissolved in water giving a solution with pH about 7. Under these conditions it is possible to precipitate the uranium as $UO_4 \cdot 2H_2O$ with hydrogen peroxide, leaving most of the fission products in solution (35). Three drops of 30% hydrogen peroxide were added and the uranium

precipitate removed by centrifuging. The supernatant liquid was evaporated to a drop and placed on the filament of the 6-inch mass spectrometer. The observed relative abundances of the cesium isotopes appear in Table VII. Other elements were found to be too contaminated to make sufficiently adequate corrections.

(ii) Treatment of Samples B and C

Samples B and C were treated in identical fashion. The outside surfaces of the quartz vials were first washed with dilute nitric acid and hydrofluoric acid, and the vials with contents then dissolved completely with 4 ml. hydrofluoric acid. Concentrated nitric acid was added to this solution and the volume reduced under a heat lamp. The resulting solution was then diluted to about 20 ml. with water and accurately weighed. This provided a stock solution of known weight, containing all the fission products, quartz and uranium.

Weighed aliquots were taken for the various analyses, which included making measurements of the relative abundances of the fission product isotopes and measurements of the isotope diluted abundances. The uranium was precipitated with hydrogen peroxide and removed in the same manner as was used for Sample A. The first attempt to locate and measure isotopic masses of Sample B revealed that both barium and strontium appear as singly charged, monofluoride ions as well as the single charged metal ions. These caused interference in the

mass ranges 107-109 and 153-157. Further aliquots were repeatedly evaporated to dryness from a strong nitric acid solution to remove the fluoride ion present in the stock before loading the filament.

(iii) Isotope Dilution

A standard isotope dilution solution, containing cesium and neodymium, was prepared. The neodymium, supplied by Research Chemicals, Inc., Burbank, California, was in the chemical form Nd_2O_3 (99.9%) and the cesium was "Specpure" CsCl , supplied by Johnson, Matthey and Co. Ltd. Appropriate portions of the dried chemicals were weighed, dissolved in nitric acid and made up to one litre. Particulars are given in Table II.

TABLE II
Isotope Dilution Solutions

Element	Chemical Form	Weight Used (gms).	No. atoms per gram solution $\times 10^{16}$
Cs	CsCl	0.01360	4.833
Nd	Nd_2O_3	0.04349	15.627

Weighed aliquots were added to weighed portions of the stock solutions. The quantities of each were so estimated that when the abundances of Nd^{142} and Nd^{143} were equal, the $\text{Cs}^{133}/\text{Cs}^{137}$ ratio would be approximately 2. This combination permits high precision measurements.

As fluorides of the rare earths are insoluble it is possible that fractionation of rare earths from the other elements could occur in the stock solution. To circumvent this, only 5.5% of the stock solution from Sample C was used for relative yield determinations, the rest being isotope diluted and treated as a single analysis. This solution was allowed to stand for several days and then evaporated to dryness and taken into solution again with nitric acid. The evaporation and dissolution were repeated twice more with final dissolution in water. Since both cesium and neodymium have only one oxidation state in solution it was assumed that isotopic equilibrium was achieved. The uranium was precipitated from the aqueous solution and the supernatant liquid concentrated for application to the filament of the 10-inch mass spectrometer. The various weights of the components involved in the isotope dilutions are contained in Table III.

TABLE III

Isotope Dilution of Samples B and C

Sample	Total Weight of Stock (gm)	Weight of Stock Diluted (gm)	Fraction of Stock Diluted	Weight of Dilution Solution added (gms)
B	16.83569	5.84451	0.3472	0.18181
C	35.28003	33.33330	0.9443	0.42442

EXPERIMENTAL RESULTS

A. Mass Discrimination

The results of the mass discrimination studies discussed in Experimental, Part A, are recorded in Tables IV and V. A large number of spectra have been averaged under various conditions and the resulting standard deviation in results is low. As no systematic variations are indicated, mass discrimination is omitted as a possible source of error in the remainder of this work. It does not, however, preclude the possibility of fractionation occurring with isotopes of other elements.

TABLE IV

Cesium Ratios as Observed on Various Collectors

Ion Detector	Filament Current (amperes)	Grid Leak (ohms)	Number of Spectra Averaged	Ratio Cs133/Cs137
Electron Multiplier	1.55	10^8	17	2.705 ± 0.028
Electron Multiplier	1.60	10^8	10	2.706 ± 0.025
Closed Slit	1.92	10^{10}	15	2.738 ± 0.023
Closed Slit	1.80	10^{10}	16	2.716 ± 0.023
Electron Multiplier	1.80	10^8	12	2.657 ± 0.033
6" Mass Spectrometer	2.00	10^9	17	2.724 ± 0.011

TABLE VNeodymium Ratios as Observed on Various Collectors

Ion Detector	Filament Current (amperes)	Grid Leak (ohms)	Number of Spectra Averaged	Ratio $\text{Nd}^{142}/\text{Nd}^{143}$
Electron Multiplier	3.05	10^8	10	0.391 ± 0.010
6" Mass Spectrometer	3.10	10^9	13	0.395 ± 0.011

B. Fission Yields of Uranium-233(a) Flux Monitoring

The total number of fissions per gram of uranium occurring in Samples B and C were determined from the results obtained from the cobalt-monitors. Table VI records the experimental data and calculated integrated flux for each sample. The flux in Sample A was not monitored.

TABLE VI

Flux Determinations with Cobalt Monitors

Sample	Cobalt Position	Observed Ion Current $\times 10^{-3}$ μ amps	Observed Ion Current From 0.150 .007 mg Standard \times 10^{-3} μ amps	Number of Atoms of Co^{60} Formed \times 10^{15}	Weight of Co^{59} at beginning (mg.)	ϕt $\times 10^{19}$
B	loose in container around vial	2.24	0.500	5.978	0.5744	2.830
		2.25	0.500	6.005	0.5734	2.848
C	loose in container on top container around vial	2.23	0.498	5.978	0.5729	2.813
		2.22	0.500	5.925	0.5729	2.812
		2.21	0.500	5.393	0.5762	2.733

* Assuming $\frac{dN^{60}}{dt} = -\lambda N^{60}$ and half-life of $\text{Co}^{60} = 5.27$ years (36).

** Assuming $N^{60} = N^{59} \sigma^{59} \phi t$ where $\sigma^{59} = 36.0 \pm 1.5$ barns (37),
 $\phi t = \text{neutrons} / \text{cm}^2$, and $t \ll \text{half-life of } \text{Co}^{60}$.

(b) Uranium

The uranium content of Sample A was 14.6% U^{233} . Samples B and C consisted of uranium isotopes U^{233} and U^{235} in the ratio 14.02 : 1 as shown in Table VII.

TABLE VII

Relative Abundances of Uranium in Samples B and C

Uranium Isotope	Relative Abundances			
	Run 1	Run 2	Run 3	Weighted Mean
238	14.6 ± 0.55	14.7 ± 0.38	13.88 ± 0.41	14.02 ± 0.14
235	< 0.01	< 0.01	< 0.01	< 0.01
233	1.00	1.00	1.00	1.00

(c) Strontium

The results of mass spectrometric analyses of the relative abundances of the strontium isotopes from fission in both samples B and C have been recorded in Table VIII, along with the time from the end of the irradiation to the time of mass spectrometric analysis.

Natural strontium contamination is indicated by the presence of mass 86, which was expected from the results of the contamination study made with the quartz. The mass 88 was corrected for the stable contribution by assuming the natural strontium abundances as given by Hier (38). The correction amounts to 14.4% in Sample B and 10.1% in Sample C. Corrections were also applied at mass 89 and 90 for decay as indicated. The half-life of Sr^{89} is not well known as three values are given in the literature, viz. 53 days (39), 54 days (41) and 55 days (42). 53 days, which is the most recent of these, was selected. The excellent agreement between samples substantiates the validity of the corrections.

TABLE VIII

Relative Fission Yields of Strontium Isotopes

Sample	Isotopic Mass	Time to Analysis (t_2) (days)	Observed Relative Abundances	Abundances Corrected For Stable Contamination *	Abundances Corrected For Decay of Sr ⁸⁹ and Sr ⁹⁰ **
B	86	106.6	0.016±0.002	0.797 0.158 1.000	0.790 0.841 1.000
	88		0.931±0.022		
	89		0.158±0.002		
	90		1.000		
C	86	126.3	0.011±0.003	0.801 0.123 1.000	0.793 0.848 1.000
	88		0.893±0.037		
	89		0.123±0.004		
	90		1.000		
				Average	
				88	0.791
				89	0.844
				90	1.000

* It is assumed that all of mass 86 is stable contamination and hence mass 88 is corrected using the natural abundances of the Sr isotopes (33).

** Assuming half-lives of 53 days (39) and 27.7 years (40) for Sr⁸⁹ and Sr⁹⁰ respectively and Equation 8, Appendix A.

(d) Yttrium

The relative abundances of Yttrium isotopes produced in U²³³ fission are given in Table IX. The corrections for holdup of Sr⁸⁹ and decay of Y⁹¹ are large and cannot be made accurately due to uncertainty in the accepted half-life values. Two values for the half-life of Y⁹¹ are given in the literature, viz. 61 days (43) and

57 days (44). The 57 day half-life was arbitrarily chosen. In spite of the high standard deviation in the individual ratios, the values obtained from the independent samples agree to 0.3%. This does not, however, preclude the possibility of more accurate results using the 61 day half-life.

TABLE IX

Relative Fission Yields of Yttrium Isotopes

Sample	Yttrium Isotopes	Time to Analysis (t_2) (days)	Observed Relative Abundances	Ratio Corrected For Holdup of Sr^{89} and Decay of Y^{91} *
B	89 91	122.5	4.54 ± 0.24 1.00	0.919 1.000
C	89 91	126.3	4.77 ± 0.12 1.00	0.914 1.000
			Average Y^{89}/Y^{91}	0.917

* Assuming Equation 12, Appendix A, and 53 days (39) and 57 days (44) respectively for half-lives of Sr^{89} and Y^{91} .

(e) Zirconium

The relative abundances of the zirconium isotopes produced in U^{233} fission are tabulated in Table X. Both yttrium and zirconium ionize as the monoxides and hence appear in the mass range 105-111. The observed mass 91, therefore, contains both zirconium and yttrium and was corrected for the latter in accordance with the yttrium ratios (Table IX). These were obtained without zirconium at a lower filament

TABLE X

Relative Fission Yields of Zirconium Isotopes in Sample B

Isotopic Mass	Observed Relative Abundance	Corrected for Yttrium*	Corrected for Stable Zr **	Corrected for Y^{91} Holdup***	Yields Reported by Steinberg (25)
89	2.307 ± 0.096				
90	4.551 ± 0.390	4.551			
91	2.264 ± 0.260	1.678	0.684	0.848	0.920
92	2.329 ± 0.061	2.329	0.819	0.319	0.944
93	1.000	1.000	1.000	1.000	1.000
94	2.392 ± 0.228	2.392	0.858	0.858	0.761
96	0.976 ± 0.051	0.976	0.733	0.733	0.790

* Ratio of $N^{89}/N^{91} = 3.938$ calculated from Equation 12, Appendix A, assuming $f^{89}/f^{91} = 0.917$ (Table IX), time of analysis (t_2) = 113 days and half-life of $Y^{91} = 57$ days.

** Assuming that all the Zr^{90} present represents stable contamination, and the natural abundances of zirconium (45).

*** 113 days after the irradiation the fraction of Zr^{91} measured is only 0.807 of the total yield of mass 91, as calculated from Equation 11, Appendix A.

temperature. Stable zirconium contamination is also present, as indicated by mass 90 since no Zr^{90} would be formed in fission. The Sr^{90} precursor to the zirconium, which has a 27.7 year half life, would not have decayed significantly in the course of 106.6 days between the irradiation and time of analysis. All masses, except mass 93, were corrected for stable contamination by using the natural abundances of zirconium reported by White and Cameron (45). Mass 91 was further corrected for Y^{91} holdup. The number of corrections in this data, as well as the uncertainty of the half-lives involved, reduce the reliability appreciably.

(f) Cerium

Cerium ionizes as the oxide and appears with neodymium in the mass range 156-160. Since it ionizes at a lower temperature than neodymium it is possible to measure the cerium abundances when the neodymium ion currents are very small. Corrections, made for the presence of neodymium as indicated by mass 143, were also small. Mass 140 is the most abundant cerium isotope in nature and, therefore, natural contamination may increase the ratio Ce^{140}/Ce^{142} . Since stable cerium contamination from the quartz was expected, the relative abundances of cerium in U^{233} fission reported by Kukavadze et al (7) were accepted. The natural abundances of cerium (46) were applied in addition to this information in order to correct the observed ratio Ce^{142}/Ce^{144} for contamination (Appendix B). Ce^{144} was also corrected for its radioactive decay. The relative cerium yields appear in Table XI.

TABLE XI
Relative Abundances of Cerium in U²³³ Fission
(Isotope Diluted Sample C)

Isotopic Mass	Observed Relative Abundances	Corrected for Nd Contamination *	Corrected for Stable Ce Contamination **	Corrected for Decay of Ce ¹⁴⁴ ***
140	1.13 ± 0.07	1.37	1.00	1.00
142	1.00	1.00	1.00	1.00
143	0.158 ± 0.008			
144	0.516 ± 0.019	0.450	0.477	0.69

* Assuming $Nd^{142}/Nd^{143} = 0.392$ and $Nd^{144}/Nd^{143} = 0.925$
 (Table XV).

** Assuming $Ce^{140}/Ce^{142} = 1.00$ in U²³³ fission (7) and natural abundances for cerium (46). The correction is carried out in Appendix B.

*** Assuming 282 day half-life for Ce¹⁴⁴ (47) and $t_2 = 129$ days in Equation 8, Appendix A.

(g) Cesium(1) Relative Yields

The relative abundances of the cesium isotopes from U^{233} fission are recorded in Table XII. Mass 135 has not been corrected for neutron capture in either this work or the published literature (26). The ratio Cs^{133}/Cs^{137} in Sample A agrees with the literature but contamination is present in Samples B and C. The results from these two samples were only used in the calculations of absolute yields of Cs^{137} since this isotope is not present in nature.

TABLE XII

Relative Fission Yields of Cesium Isotopes

Sample	Isotopic Mass	Observed Relative Abundance	Corrected For Decay of Cs^{137} **	Published Results (26)
A	133	0.967 ± 0.010	0.872	0.870
	135	$0.653 *$		$0.689 *$
	137	1.000	1.000	1.000
B	133	1.003 ± 0.009	0.994	
	135	0.450 ± 0.003		
	137	1.000	1.000	
C	133	1.020 ± 0.004	1.009	
	135	0.458 ± 0.005		
	137	1.000	1.000	

* Not corrected for neutron capture and hence these yields are minimum values.

** Assuming $t_2 = 1436$ days, 130 days and 149 days for Samples A, B and C respectively, the half-life for $Cs^{137} = 26.6$ years (45) and Equation 8, Appendix A.

(ii) Absolute Yields

Table XIII lists the results obtained for the $\text{Cs}^{133}/\text{Cs}^{137}$ ratio after isotope dilution. The weights of reagents involved (Tables II and III), the flux (Table VI) and these ratios are combined in Equation 17, Appendix C to give the absolute yield of the 137 mass chain. The deviation from the average of Samples B and C is less than 1%. Therefore, the relative yield of mass 133 reported in Table XII is also made absolute.

TABLE XIIIIsotope Dilution Data for Cesium

Sample	Isotopic Mass	Observed Abundance	Corrected for Decay of Cs^{137} *	Number of Atoms Cs^{137} in Sample $\times 10^{16}$	Absolute Fission Yield of Cs^{137} ** (%)
B	133 137	2.856 ± 0.040 1.000	2.827 1.000	1.3954	6.55
C	133 137	2.717 ± 0.020 1.000	2.688 1.000	1.3065	6.41
Average					6.48 ± 0.07

* Assuming half-life of $\text{Cs}^{137} = 26.6$ years (48) and $t_2 = 119$ days 128 days respectively in Equation 8, Appendix A.

** Assuming Equation 17, Appendix C.

(h) Neodymium

(i) Relative Yields

The relative fission yields of the neodymium isotopes produced in U^{233} fission are recorded in Table XIV.

Corrections were made for cerium contamination, natural neodymium contamination and holdup due to cerium at mass 144. It was also necessary to correct mass 150 for a contribution of Sm^{150} resulting from neutron capture by Sm^{149} . The results are in good accord with those published by Melaiika et al (29). A typical fission spectrum of neodymium is illustrated in Figure 7.

(ii) Absolute Yields

The ratio of masses 142 : 143 after isotope dilution appears in Table XV. Mass 142 was corrected for cerium contamination, using the data in Table XI. The weights of isotope dilution solution and the fraction of stock diluted (Table III) as well as the flux (Table VI) and the neodymium ratios were combined in Equation 17, Appendix C, to obtain the absolute fission yield of mass 143. Absolute yields were therefore assigned to masses 144, 145, 146, 148 and 150 by comparing the relative neodymium ratios (Table XIV) to this absolute value.

TABLE XIV

Relative Fission Yields of Neodymium Isotopes

Sample	Isotopic Mass	Observed Relative Yields	Corrected for Ce Contamination *	Corrected for Nd Contamination **	Corrected for Decay of Ce ¹⁴⁴ and Sm ¹⁵⁰ ***	Values from Literature (29)
B	140	0.053 ± 0.001				
	142	0.074 ± 0.001	0.035			
	143	1.000	1.000	1.000	1.000	1.000
	144	0.271 ± 0.003	0.254	0.217	0.764	0.779
	145	0.579 ± 0.003	0.579	0.578	0.578	0.587
	146	0.454 ± 0.003	0.454	0.439	0.439	0.441
	148	0.221 ± 0.002	0.221	0.227	0.227	0.224
	149	0.007 ± 0.0004	0.007	0.008		
	150	0.103 ± 0.001	0.103	0.098	0.088	0.089
C	140	0.030 ± 0.002				
	142	0.092 ± 0.001	0.034			
	143	1.000	1.000	1.000	1.000	1.000
	144	0.302 ± 0.003	0.276	0.249	0.755	0.779
	145	0.583 ± 0.003	0.583	0.582	0.582	0.587
	146	0.455 ± 0.003	0.455	0.441	0.441	0.441
	148	0.227 ± 0.002	0.227	0.223	0.223	0.224
	149	0.0045 ± 0.0006	0.0045	0.0046		
	150	0.101 ± 0.001	0.101	0.095	0.089	0.089
Average	143				1.000	1.000
	144				0.770	0.779
	145				0.580	0.587
	146				0.440	0.441
	148				0.225	0.224
	150				0.089	0.089

* Assuming $Ce^{140}/Ce^{142} = 1.37$ and $Ce^{140}/Ce^{144} = 3.04$ (Table XI)

** Assuming all Nd^{142} is stable contamination and using the natural abundances for neodymium (49).

*** Assuming 282 day half-life for Ce^{144} (47), $t_2 = 111$ days and 126.3 days respectively for Samples B and C and Equation 11, Appendix A. Also assuming $Sm^{150}/Sm^{149} = 1.25$ (Table XVI).

FIGURE 7 : TYPICAL MASS SPECTROGRAM OF NEODYMIUM

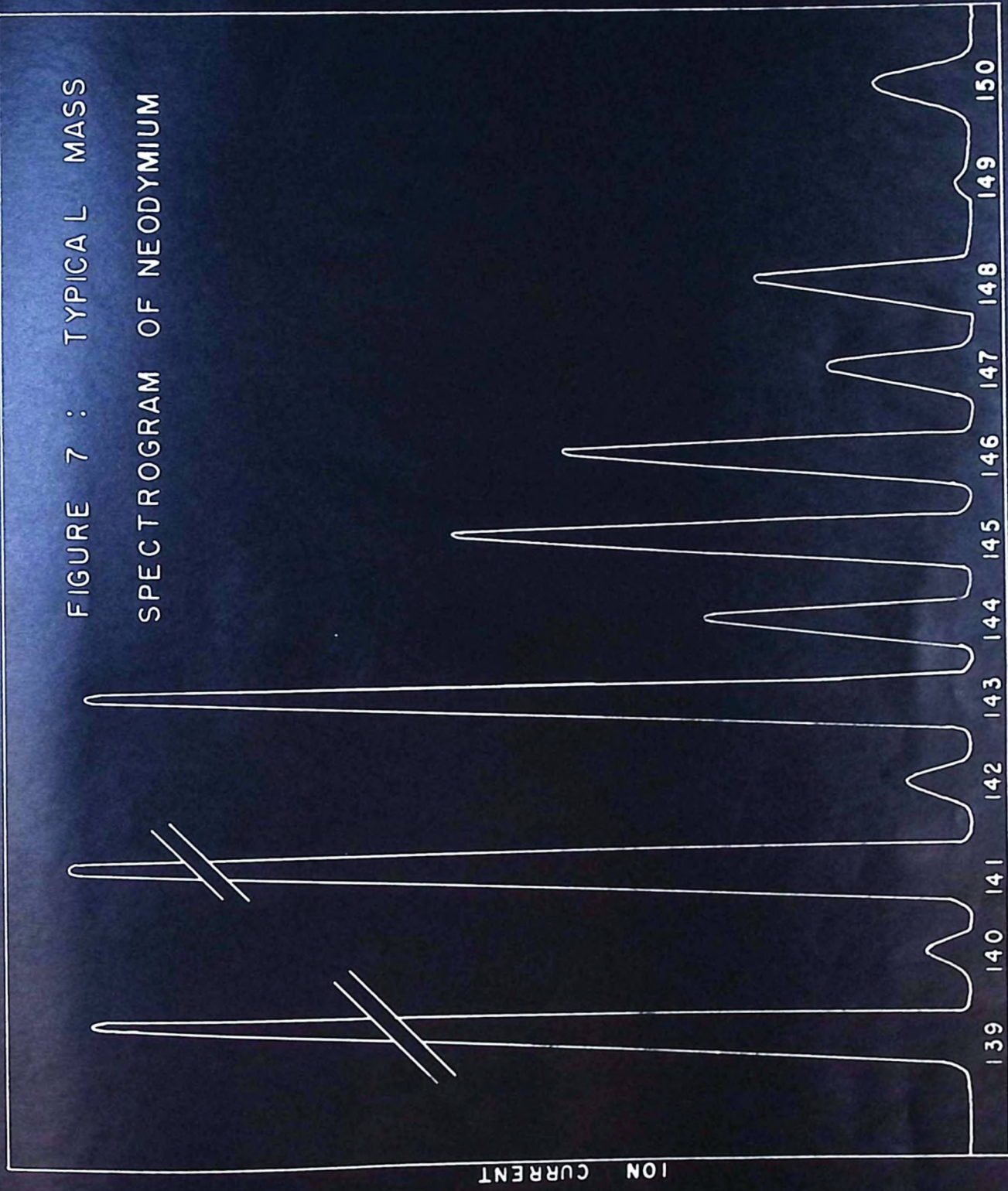


TABLE XV

Isotope Dilution Data for Neodymium in Sample C

Isotopic Mass	Observed Relative Abundance	Corrected for Ce Present *	Number of Atoms Nd ¹⁴³ in Sample $\times 10^{16}$	Absolute Fission Yield of Mass 143 (%)
140	0.026 \pm 0.0003			
142	0.911 \pm 0.010	0.892		
143	1.000	1.000	1.308	6.41
144	0.925 \pm 0.011			

* Assuming observed value 1.37 for the ratio of Ce¹⁴⁰/Ce¹⁴² (Table XI).

(1) Samarium

Samarium was observed as the singly charged metal ions. Mass 154 is not included in these observations as it could not be corrected for the Da¹³⁵ F¹⁹ ion contribution. The relative abundances of the other masses and the corrections applied are given in Table XVI.

The agreement with the values previously reported (29) is considered excellent except at mass 147. The value given in the literature for this yield is thought to be large due to a contribution from Pm¹⁴⁷.

TABLE XVI
Relative Abundances of Samarium Isotopes
in U²³³ Fission (Sample B)

Isotopic Mass	Observed Mass Spectrometric Ratio	Corrected for Hold-up of Pm ¹⁴⁷ *	Corrected for Neutron Capture **	Normalized	Literature Values (29)
147	10.85 ± 0.69	111.40	111.40	2.357	2.81
149	20.93 ± 0.43	20.93	47.09	1.000	1.00
150	26.16 ± 0.39	26.16	0.00	0.000	0.00
151	17.67 ± 0.52	17.67	20.15	0.423	0.422
152	15.97 ± 0.51	15.97	13.49	0.286	0.278
154	not measured ***				0.061

* Assuming 2.52 year half-life of Pm¹⁴⁷ (29), $t_2 = 136$ days and Equation 11, Appendix A.

** Assuming equations given by Melaiika et al (29).

*** BaF⁺ ions were contributing at masses 153 and 154.

DISCUSSION

The experimentally determined yields of strontium, yttrium and zirconium isotopes taken from Tables VIII, IX and X are summarized in Table XVII along with previously published yields for the fission of U^{233} . Since only relative yields of these elements have been measured in this work, they have been placed on an absolute basis by normalization to the 7.10% yield of the mass 93 chain reported by Steinberg (24).

These fission yields are less reliable than those of the heavy fragment distribution discussed below. The reason for reporting these yields, however, is the unique manner in which the strontium and zirconium yields have been normalized to each other. It is apparent from Table XVII that the relative yields of Y^{89} and Y^{91} (Table IX) allow the normalization of the relative strontium yields (Table VIII) to those of zirconium (Table X). By this means it is, therefore, possible to place all the yields of mass chains 88 - 96 on an absolute basis by determining a single absolute yield in this mass region.

Experimental difficulty was experienced during the mass spectrometric analysis of the zirconium isotopes since ions were not produced in sufficient numbers to give large ion currents in comparison with the background noise of the instrument. Furthermore, if the strontium fluoride ion were present it would enhance the

TABLE XVII

Fission Yields of Light Fragments Formed in the Thermal
Neutron Fission of U²³⁵

Mass Chain	Element Involved	U ²³⁵ Fission Yields (%)			
		This Work	Interpolated or Extrapolated	Values from Literature	Reference
75 - 78			0.25		
79			0.30		
80			0.44		
81			0.62		
82			0.84		
83	Kr			1.14	(26)
84	Kr			1.90	(26)
85	Kr			2.49	(26)
86	Kr			3.18	(26)
87			4.19		
88	Sr	5.17			
89	Sr - Y	5.52		6.50	(25)
90	Sr	6.54			
91	Zr - Y	6.02		6.53	(24)
92	Zr	5.81		6.70	(24)
93	Zr	7.10		7.10	(24)
94	Zr	6.09		6.02	(24)
95	Mo			6.10	(24)
96	Zr	5.20		6.10	(24)
97	Mo			5.35	(24)
98	Mo			5.18	(24)
99	Mo			5.10	(24)
100	Mo			4.40	(24)
101	Ru			3.00	(24)
102	Ru			2.37	(24)
103	Ru			1.60	(24)
104	Ru			0.96	(24)
105			0.54		
106	Ru			0.28	(24)
107			0.04		
108 - 115			0.15		
Summation		47.45	7.37	82.8	

Summation of Yields:

This Work	47.45
From Smooth Curve	7.37
Others From Literature	43.05
Total	<u>97.87</u>

yields of masses 107 and 109 corresponding to Zr^{91} and Zr^{93} .

The presence of these ions cannot be precluded since they occur at the masses with yields which deviate the most. It is impossible to correct the measured values for their presence since both the strontium isotopes occur at the same mass numbers as the zirconium isotopes. Uncertainty in the half-life of Y^{91} contributes another source of error to the mass 91 yield. Because of these difficulties it is doubtful whether one should consider the relative yields significantly different from those given by Steinberg (Table XVII).

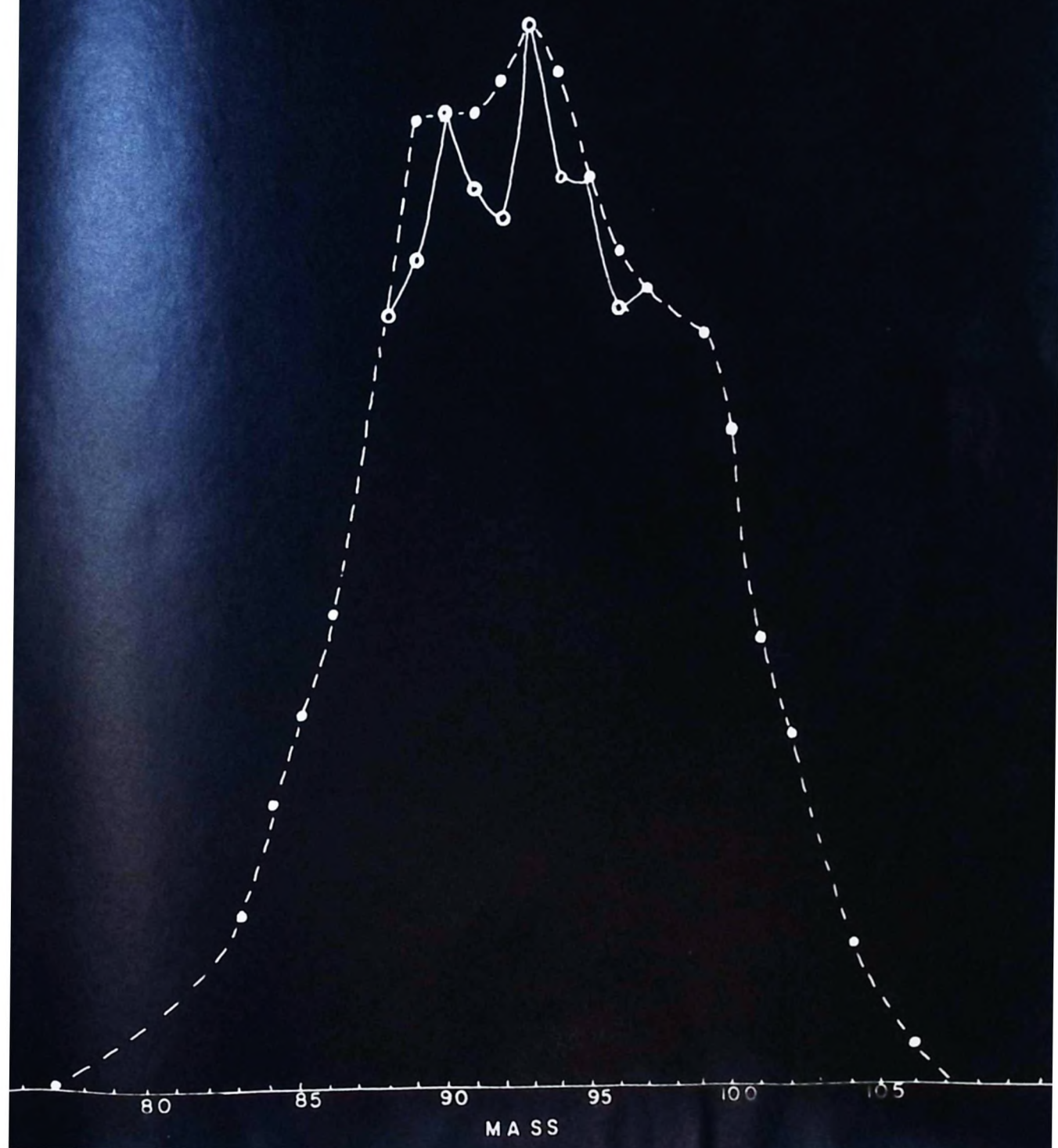
Independent determinations of the relative strontium yields which are shown in Table VIII were reproducible to 1%. Since these yields have not previously been reported these data may be considered as a significant contribution to the knowledge of fission yields in the light mass region of the mass-yield distribution.

Although independent determinations of the relative yields of Y^{39} and Y^{91} agree to 0.4%, the values are strongly dependent on the half-lives of Sr^{39} and Y^{91} . Until reliable values of these half-lives are known it will be difficult to assess the accuracy with which the yields of the strontium isotopes have been normalized to those of the zirconium isotopes.

The fission yield values (Table XVII) have been plotted in Figure 8 along with the values compiled by Katcoff (6). It must be pointed out, however, that only one absolute yield, that of mass 99, has been determined in this light mass region. Other yields were selected by Katcoff in such a manner that their total sum was 100%. Since many of these yields were obtained by interpolation (such as the

FIGURE 8 : LIGHT MASS DISTRIBUTION
FROM U²³³ FISSION

○ THIS WORK
● LITERATURE



mass 87 - 90 region) the appearance of fine structure is excluded. The apparent fine structure indicated by the present work, as well as its differences from the published work, as shown in Figure 8, cannot be considered significant because of the many uncertainties. In spite of these, however, it is apparent that the most probable yield of the light mass distribution occurs at mass 93. This is, therefore, two mass units lower than the corresponding yield in U^{235} fission (6), and verifies Steinberg's report (15) in contrast to the early work of Grunmitt (14).

It should be noted that the contributions of the delayed neutrons have not been included in either the published or present data given in Table XVII. About 0.755 per cent of the 2.5 neutrons per fission are emitted by fission fragments after one or more beta decays have occurred. In the light mass distribution Br^{87} , Br^{89} and Br^{91} are known delayed neutron emitters (50). This report predicts that the observed cumulative fission yields of the end product member of the mass 87 chain would be decreased by 0.052 fission yield per cent while the yield of the mass 86 chain would be raised by a similar amount as a result of neutron emission by Br^{87} . Likewise the mass 89 and 91 chains are decreased by 0.23 per cent and the mass 88 and 90 chains increased by this amount. Figure 8 illustrates that consideration of the delayed neutrons would tend to smooth out the pronounced spike at mass 90, without affecting the valley at mass 92. There are, however, several delayed neutron emitters that have not yet been associated with a given mass chain which could influence these yields.

Further work is being carried out in this laboratory to improve the techniques for analysing zirconium and yttrium mass spectrometrically. The author found that zirconium ions would not form until a relatively high filament temperature was reached and the sample was soon lost at this temperature. The solution to the problem, therefore, may involve the application of the three-filament source. The sample may then be evaporated at a lower temperature from the side filaments and ionized on the hotter central filament. The general procedure as outlined above should prove to be important in assigning the absolute fission yields to the light mass distribution.

The cesium, neodymium and cerium fission yields taken from Tables XIII, XV and XI respectively are summarized in Table XVIII, along with the literature values compiled by Katcoff. The cesium yield is the average of two entirely independent determinations which agree to within 1%. The accuracy of these values is, therefore, considered to be better than 3 per cent. The relative yields of the Cs¹³³ and Cs¹³⁷ agree well with those reported by Fleming et al (26), but no absolute fission yields in this mass region have previously been reported. The cesium and xenon values assigned by Katcoff were only placed in relation to the absolute neodymium and cerium yields of Kukavadsze et al (7) in such a manner that the summation of the yields in the heavy mass distribution was 100%.

The neodymium yields are based on a single determination, but both the fission product ratios and the ratios after isotope dilution were determined by two mass spectrometers which give an overall precision to the value of ±1.0 per cent. These values are therefore

TABLE XVIII

Absolute Fission Yields of Heavy
Fragments Formed in the Thermal
Neutron Fission of U²³³

Mass Chain	Element Involved	U ²³³ Fission Yields (%) *			
		This Work	Interpolated or Extrapolated	Values from Literature	Reference
117 - 129			2.34		
130			2.00		
131	Xe	3.30		3.74	(26)
132	Xe	4.52		5.10	(26)
133	Cs	5.64		6.13	(6)
134	Xe	5.30		6.54	(26)
135	Cs	4.46		> 4.9	(6)
136	Xe	7.85		< 8.9	(6)
137	Cs	6.48		7.16	(6)
138	Ba		6.72		
139	La		6.96		
140	Ce	7.16		5.6	(7)
141	Pr		7.16		
142	Ce	7.16		5.6	(7)
143	Nd	6.41		5.2	(7)
144	Nd - Ce	4.94		4.0	(7)
145	Nd	3.76		3.0	(7)
146	Nd	2.33		2.3	(7)
147	Sm	2.08		1.71	(6)
148	Nd	1.43		1.15	(7)
149	Sm	0.88		0.61	(6)
150	Nd	0.57		0.43	(7)
151	Sm	0.43		0.26	(6)
152	Sm	0.29		0.17	(6)
153			0.12	0.095	(6)
154	Sm	0.05		0.037	(6)
155 - 162			0.20		
Summation		76.04	25.50	72.73	

Summation of Yields:

This Work 76.04
From Smooth Curve 25.50
Total 101.54

* The actual flux is less in the sample than in the cobalt monitor by 1.0% (Appendix D), because of self-shielding of the U²³³. This necessitates the raising of all yields reported here by this amount. Since the total of the fission yields must also equal 100% this correction is not made.

expected to have about equivalent absolute accuracy to the cesium yields.

In order to obtain the yields of the 140 and 142 mass chains relative to the 144 mass chain the relative abundances of the cerium isotopes were utilized. Since the measured ratios of these isotopes were influenced by natural cerium contamination from the quartz vial the relative yields of Ce^{140} and Ce^{142} obtained by Kukavadze et al (7) have been assumed. The error from the resulting correction would probably be small, however, since only about 3 per cent of the measured 142 mass chain was found to be natural cerium contamination (Appendix B). The largest error in normalizing the cerium yields to those of neodymium probably resulted from the correction of the 144 mass chain for the partial radioactive decay of the cerium. The Ce^{140} and Ce^{142} yields relative to the neodymium yields are probably accurate to within 2% and will therefore, have absolute accuracy of about 5%.

The samarium yields were only determined on a relative basis but masses 147, 149 and 151 are flanked by neodymium at masses 146, 143 and 150. The data in Table XVIII has been obtained by assigning absolute values to the relative samarium fission yields from Table XVI such that a smooth fission yield curve resulted. As the same values are obtained by interpolation at three different points no serious error is expected.

The neodymium and cerium yields reported by Kukavadze et al (7) and the Ba^{140} yield reported by Steinberg (15) are the only absolute fission yields given in the literature for the heavy mass distribution of U233. Kukavadze et al (7) obtained yields of 5.6% and 5.2% for the 140 and 143 mass chains respectively, whereas Steinberg (15) obtained 6.0% for the former. Katcoff (6), after selecting the 140 yield given

by Steinberg in preference to that of Kukavacze, accepted these known values in order to assign yields to the remaining isotopes. This was done arbitrarily in such a manner that the yields from the entire distribution added to 100 per cent.

The Russian investigators worked with large quantities of fission products and, therefore, it is logical to assume that their relative mass spectrometric ratios are reliable. Indeed, they agree with the yields reported by Melaiika et al (29) and the present work except at mass 144 where apparently they have made no correction for Ce^{144} decay. The method used to determine the number of fissions, however, is questionable. Can kilocuries of fission products be chemically separated from uranium so completely that accurate changes in the weight of uranium could be detected? Lack of experimental details makes it difficult to assess whether some twenty-five fission product elements could be separated from a total of 60 mg. of U^{235} without the loss of sub-milligram quantities of the latter.

Steinberg, on the other hand, quotes an accuracy of 15 per cent for the Ba^{140} yield, i.e. $6.0 \pm 0.9\%$. This is less than the 7.1 ± 0.4 per cent value from this work but is not inconsistent with its accuracy. The difference is significant, however, as Katcoff related all other fission yields to this specific value. In order to achieve a 100% summation of the fission yields Katcoff was forced to assign high relative values to the cesium and xenon yields and accept the low values for the neodymium yields.

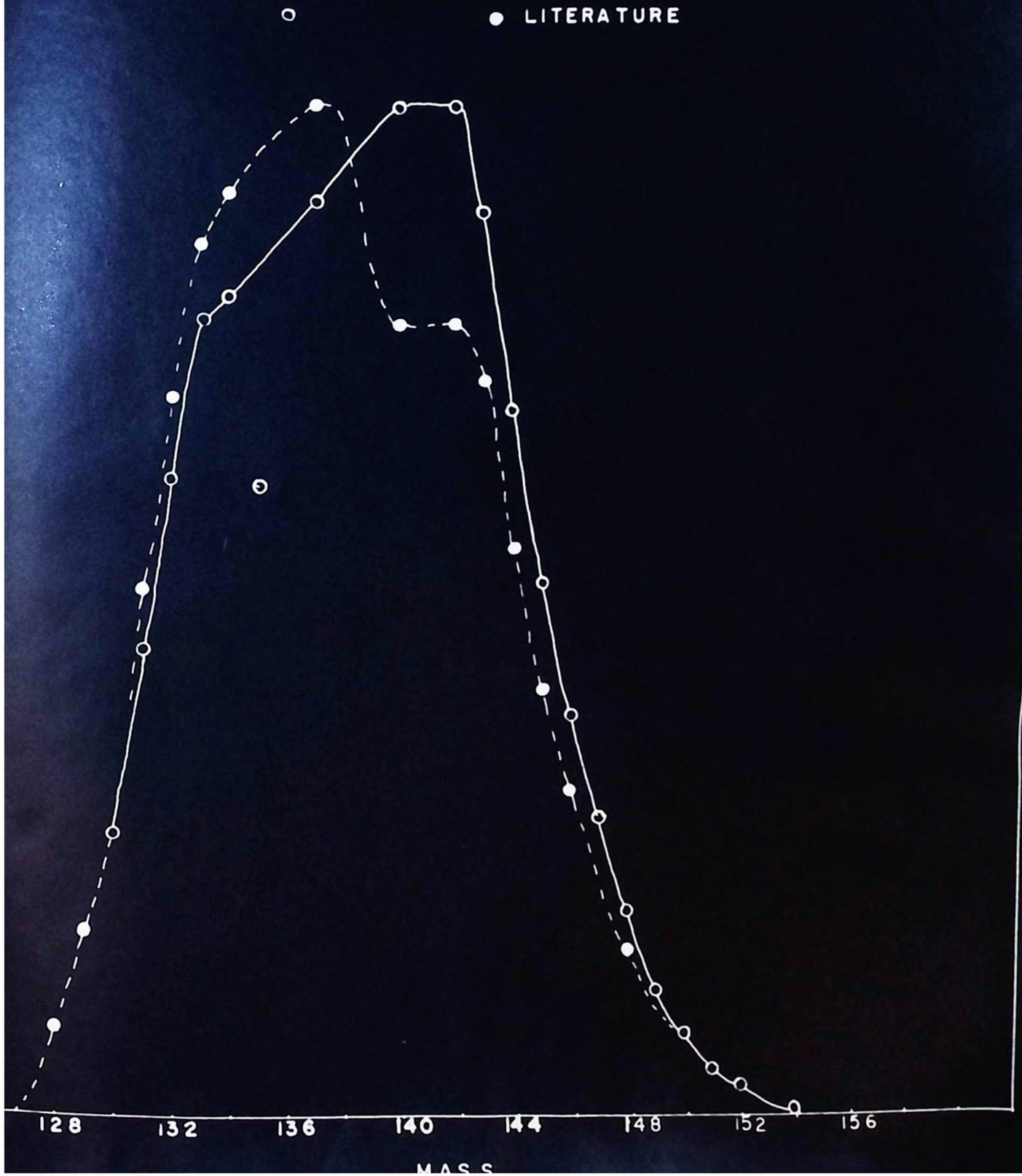
This work has assigned absolute values to both the cesium and neodymium isotopes, thus fixing both sides of the heavy mass

distribution. It can be seen in Figure 9 that the cesium yields are actually lower than the arbitrary designation given by Katcoff, whereas the neodymium yields are greater.

There is strong evidence to select the distribution reported here in preference to that derived by Katcoff. In addition to assigning values on both sides of the mass-yield distribution thus avoiding serious errors in extrapolation, a large fraction of the total distribution has been determined. As shown in Table XVIII 76.04% of the fission yields are given absolute values. Another 20.84% of the fission yields result from the interpolation of yields at masses 133, 139 and 141 from a smooth curve. By including extrapolated values from the wings a total summation of 101.54% was obtained. This is the best possible verification for a fission yield assignment, as the yields were not forced to add to 100 per cent as in Katcoff's compilation. It is therefore estimated that the absolute fission yields reported in Table XVIII are accurate to $\pm 3\%$.

The graphical representation is a smooth mass-yield curve (Figure 9) with no apparent fine structure except possibly at masses 135 and 136 where no attempt was made to correct for neutron capture and at masses 137, 139 and 141 which were interpolated. The yields at masses 135 and 136 should be assigned from analysis of a sample irradiated with a low neutron flux, as the correction for neutron capture would be much smaller. This lack of fine structure is in apposition to the theory of Pappas (23), which predicted fine structure at masses 134 and 135 for U^{233} fission. The distribution is non-symmetrical and the most probable yield is found at mass 141.

FIGURE 9 : HEAVY MASS DISTRIBUTION FROM

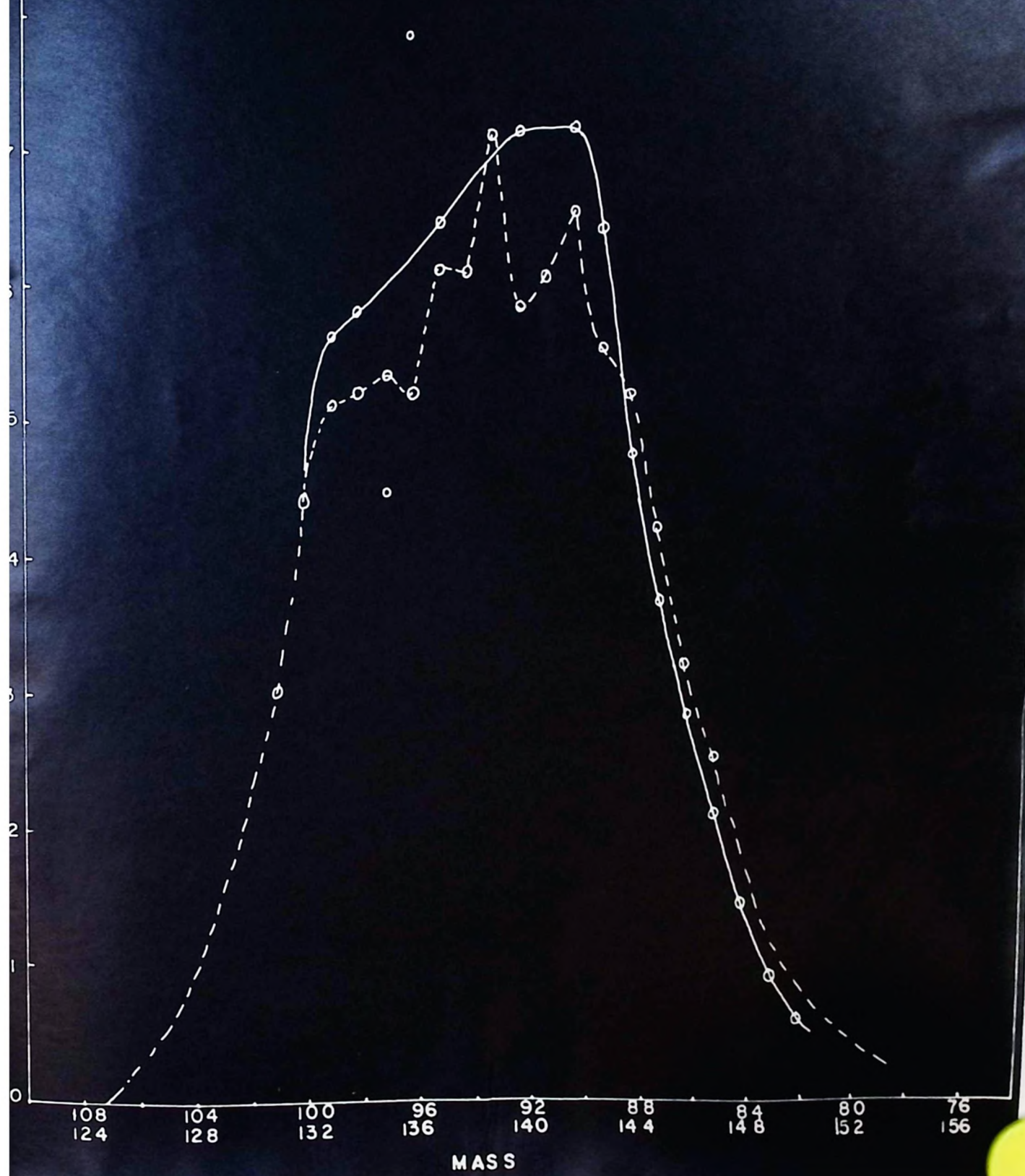
 U^{233} FISSION○ THIS WORK
● LITERATURE

Any structural preference in binary fission must result in equal yields of complementary fragments, and hence if both fragments de-excite by the loss of the same number of neutrons, the observed fission yields must be identical. The asymmetrical fission yield curve is a general manifestation of this. Neutron emission from the primary fission fragments, delayed neutron emission from fission products which have undergone one or more β decay processes and neutron capture by fission products all increase the yield of a given mass at the expense of the yield of some other mass. These three factors affect the yields of any one particular distribution without affecting the yield of the complementary mass chain and results in the characteristic peculiarities of each distribution.

These factors can be assessed by folding the fission yield curves over each other as shown in Figure 10. The yields of the light mass chains have been plotted to correspond to the heavy mass chain such that their combined masses total 232. The sum of the mass numbers of corresponding fission fragments, together with the number of emitted neutrons, must be 234 ($U^{233} + 1$ neutron), and it is assumed that most fission fragments de-excite by the loss of at least one prompt neutron.

The large number of possible errors in the fission yields of the light mass distribution make interpretation of post fission effects from the differences between the light and heavy distribution very difficult. It is worth noting, however, that the light mass distribution appears slightly wider than that of the heavy mass fragments, just as was observed in U^{235} fission plots (51). Delayed

MASS YIELDS IN THE THERMAL
NEUTRON FISSION OF U^{233}



neutron emitters can account for the other differences in these distributions.

The general shape of this heavy mass distribution for U²³³ resembles that of Pu²³⁹ (52). Since both U²³³ and Pu²³⁹ have similar neutron to proton ratios it is suggested that this may be the important nuclear constant in determining the shape of the mass-yield distribution.

BIBLIOGRAPHY

- (1) Fermi, E.; *Nature* 133, 893 (1934).
- (2) Curie, I., and Savitch, P.; *J. de phys.* (7) 2, 355 (1938).
- (3) Hahn, O., and Strassmann, F.; *Naturwiss.* 27, 11 (1939).
- (4) Meitner, L., and Frisch, O.R.; *Nature*, 143, 239 (1939).
- (5) Alichanov, A.I., Wladimirovsky, W.W., and Wikipin, S.J.; Paper No. 653, International Conference on the Peaceful Uses of Atomic Energy, Geneva, Switzerland, (1955).
- (6) Katcoff, S.; Handbook of Nuclear Engineering. Addison-Wesley (1956).
- (7) Kukavadze, G.M., Anikina, M.P., Goldin, L.L., and Erebler, B.V.; Moscow Conference of the Peaceful Uses of Atomic Energy (July 1955).
- (8) Katcoff, S., and Rubinson, W.; *Phys. Rev.* 91, 1453 (1953).
- (9) Yaffe, L., Thode, H.G., Merritt, W.F., Hawkins, R.C., Brown, F., and Bartholomew, R.H.; *Can. J. Chem.* 32, 1017 (1954).
- (10) Petruska, J.A., McLaika, E.A., and Tomlinson, R.H.; *Can. J. Physics* 33, 640 (1955).
- (11) Seaborg, G.T., Coifman, J.W., Stoughton, R.W.; *Phys. Rev.* 71 378, (1947).
- (12) Hagemann, F., Katzin, L.I., Studier, M.H., Ghiorso, A., and Seaborg, G.T.; *Phys. Rev.* 72, 252 (1947).
- (13) English, A.C., Cranshaw, T.E., Demars, P., Harvey, J.A., Hincks, E.P., Jelley, J.V., May, A.H.; *Phys. Rev.* 72, 253 (1947).
- (14) Crummitt, W.E., and Wilkinson, G.; *Nature* 161, 520 (1948).
- (15) Steinberg, E.P., Seiler, J.A., Goldstein, A., Dudley, A.; MDEC 1632, United States Atomic Energy Commission (1947).
- (16) Deutsch, H., and Ramsey, M.; Plutonium Project Report, EA-510, (1946).

- (17) Stanley, C.W., and Katcoff, S.; *J. Chem. Phys.* 17, 653 (1949).
- (18) Coryell, C.D. and Sugarman, H.; *Natl. Nuclear Energy Ser.*, Vol. 9. (1951).
- (19) Thode, H.G., and Graham, R.L.; *Can. J. Research A* 25, 1, (1947).
- (20) Macnamara, J., Collins, C.B., and Thode, H.G.; *Phys. Rev.* 78, 129 (1950).
- (21) Wilos, D.R., Smith, B.W., Morsley, A., and Thode, H.G.; *Can. J. Physics* 31, 419 (1953).
- (22) Melaika, E.A.; M.Sc. Thesis, McMaster University (1954).
- (23) Inghram, M.G.; *Ann. Rev. Nuc. Science*, 4, 81 (1954).
- (24) Steinberg, E.P., Glendenin, L.E., Inghram, M.G., and Hayden, R.J.; *Phys. Rev.* 95, 867 (1954).
- (25) Steinberg, E.P., and Glendenin, L.E.; Paper No. 614, International Conference on the Peaceful Uses of Atomic Energy, Geneva, Switzerland (1955).
- (26) Fleming, W., Tomlinson, R.H., and Thode, H.G.; *Can. J. Physics* 32, 522 (1954).
- (27) Glendenin, L.E.; Ph.D. Thesis, Massachusetts Institute of Technology, (1949).
- (28) Pappas, A.C.; Lab. for Nuclear Science Tech. Rept. No. 63, Massachusetts Institute of Technology, (1953).
- (29) Melaika, E.A., Parker, H.J., Petruska, J.A., and Tomlinson, R.H.; *Can. J. Chem.* 33, 830 (1955).
- (30) Graham, R.L., Harlness, A.L., and Thode, H.G.; *J. Sci. Instruments*, 24, 119 (1947).
- (31) Inghram, M.G.; *Rev. Sci. Instruments*, 24, 58 (1953).
- (32) Inghram, M., and Hayden, R.; Handbook of Mass Spectroscopy, (1952).
- (33) Allen, J.S.; *Rev. Sci. Instruments*, 13, 739 (1947).
- (34) Fero, J.A., and Rowen, W.H.; Tech. Rept. No. 6, Laboratory for Nuclear Science and Engineering, M.I.T., (1947).
- (35) Petruska, J.A.; M.Sc. Thesis, McMaster University (1954).

- (36) Tobailen, J.; *Compt. rend.* 233, 1360 (1951).
- (37) Hughes, D.J., and Harvey, J.A.; Neutron Cross Section Advisory Group, BNL 325, (1955).
- (38) Hier, H.O.; *Phys. Rev.* 54, 275 (1938).
- (39) Wiles, D.M., and Tomlinson, R.H.; *Can. J. Physics* 33, 133 (1955).
- (40) Novey, T.B., Engelkeimer, D.W., Brady, E.L., and Glendenin, L.E.; *MNES-PPR* 2, 678 (1951).
- (41) Lieber, C.; *Naturwiss.* 27, 421 (1939).
- (42) Stewart, D.M.; *Phys. Rev.* 56, 629 (1939).
- (43) Langer, L.M., and Price, H.C.; *Jr. Phys. Rev.* 76, 641 (1949).
- (44) Joliot, F.; *Comp. rend.* 218, 733 (1944).
- (45) White, J.R., and Cameron, A.H.; *Phys. Rev.* 74, 991 (1948).
- (46) Inghram, H.G., Hayden, R.J., and Hess, D.C., Jr.; *Phys. Rev.* 72, 967 (1947).
- (47) Schuman, R.P., and Camilli, A.; *Phys. Rev.* 81, 158 (1951).
- (48) Wiles, D.M., and Tomlinson, R.H.; *Phys. Rev.* 99, 188 (1955).
- (49) Inghram, H.G., Hess, D.C. Jr., and Hayden, R.J.; *Phys. Rev.* 74, 98 (1948).
- (50) Clarke, R.L.; Symposium on the Physics of Fission, Chalk River, (1956).
- (51) Petruska, J.A., Thode, H.G., and Tomlinson, R.H.; *Can. J. Physics* 33, 693 (1955).
- (52) Wiles, D.M., Petruska, J.A., and Tomlinson, R.H.; *Can. J. Chem.* 34, 227 (1956).
- (53) Case, K.M., de Hoffmann, P., and Placzek, G.; Introduction to the theory of neutron diffusion. Vol. 1. U.S. Government Printing Office, Washington, D.C. (1953).

APPENDIX A

The Equations for Converting Mass Spectrometric Ratios to Cumulative Fission Yields

(a) Correction for Radioactive Decay

When the ratio of two isotopes, one of which is radioactive, is measured with the mass spectrometer, it must be corrected for the decay of the radioactive species so that the ratio will represent the fission yields.

If the rate of formation of mass chain x is

$$\frac{dN_x}{dt} = N_u \sigma_u \phi f_x \quad (1)$$

where $\frac{dN_x}{dt}$ = increase in the number of atoms of x per unit time,

N_u = number of atoms of uranium present,

σ_u = fission cross section of uranium for thermal neutrons,

ϕ = neutron flux (neutrons /cm²),

f_x = the fission yield of mass chain x .

and the rate of disintegration is

$$\frac{dN_x}{dt} = - N_x \lambda_x \quad (2)$$

where λ_x = decay constant of radioactive species x , then from equations

(1) and (2) the net rate of formation is

$$\frac{dN_x}{dt} = N_u \sigma_u \phi f_x - N_x \lambda_x \quad (3)$$

which may be solved to give

$$N_x = \frac{N_u \sigma_u \phi f_x}{\lambda_x} \left(1 - e^{-\lambda_x t_1} \right) \quad (4)$$

where t_1 = time during which irradiation was carried out.

If a time t_2 elapses from the end of irradiation to the time of analysis, the species x will have decayed by an amount $e^{-\lambda_x t_2}$.

Then

$$N_x = \frac{N_u \sigma_u \phi f_x}{\lambda_x} \left(1 - e^{-\lambda_x t_1} \right) e^{-\lambda_x t_2} \quad (5)$$

If N_y is the total yield of atoms of a stable end product, i.e.

$\lambda_y \ll 1$, then

$$N_y = N_u \sigma_u \phi t_1 f_y \quad (6)$$

The observed mass spectrometric ratio of N_x/N_y at t_2 is

$$\frac{N_x}{N_y} = \frac{f_x}{\lambda_x f_y t_1} \left(1 - e^{-\lambda_x t_1} \right) e^{-\lambda_x t_2} \quad (7)$$

whence the fission yield ratio of a stable end product to a radioactive end product is

$$f_y/f_x = \frac{N_y}{N_x} \left[\frac{1}{\lambda_x t_1} \left(1 - e^{-\lambda_x t_1} \right) e^{-\lambda_x t_2} \right] \quad (8)$$

Equation (8) is applicable to the ratios of Ce^{142}/Ce^{144} , Sr^{88}/Sr^{89} , Sr^{88}/Sr^{90} and Cs^{133}/Cs^{137} .

(b) Correction for Radioactive Holdup

When the ratio of two isotopes, both of which are stable, is measured with the mass spectrometer, and one of the isotopes, Z , is being formed by the decay of a long lived parent, x , the ratio must be corrected by the amount of the stable isotopes not yet produced at time of analysis, t_2 .

At time t_2 the amount of parent present is given by equation (5), but the total yield of the chain is $N_u \sigma_u \phi t_1 f_z$. Hence the amount of stable daughter present at time t_2 is

$$N_z = N_u \sigma_u \phi f_z \left[t_1 - \frac{1}{\lambda_x} \left(1 - e^{-\lambda_x t_1} \right) e^{-\lambda_x t_2} \right] \quad (9)$$

If N_y represents the number of atoms of some other stable isotope, then N_y is given by equation (6).

The observed ratio is given by

$$N_z/N_y = \frac{f_z}{f_y} \left[1 - \frac{1}{\lambda_x t_1} \left(1 - e^{-\lambda_x t_1} \right) e^{-\lambda_x t_2} \right] \quad (10)$$

whence the fission yield ratio of the stable isotope to the stable daughter with the long lived parent is

$$\frac{f_y}{f_z} = \frac{N_y}{N_z} \left[1 - \frac{1}{\lambda_x t_1} \left(1 - e^{-\lambda_x t_1} \right) e^{-\lambda_x t_2} \right] \quad (11)$$

Equation (11) is applicable to the ratios $\text{Nd}^{143}/\text{Nd}^{144}$, $\text{Sm}^{149}/\text{Sm}^{147}$ and $\text{Zr}^{93}/\text{Zr}^{91}$.

(c) Correction Applied to the Ratio of an Isotope being Formed and
and Isotope Decaying Away

Consider the case where one member, z , of a measured mass spectrometric ratio is the stable end product of a long live parent and the other member, x , is a radioactive nuclide with half-life sufficiently long to enable its yield to be measured on the mass spectrometer. Then the number of atoms of z present at the time t_2 , N_z , is given by equation (9) and the number of atoms of x , N_x , by equation (5). The ratio of the yields of x and z can be obtained from the

ratio of the equations whence

$$\frac{f_x}{f_z} = \frac{N_x}{N_z} \left[\frac{t_1 - \frac{1}{\lambda_z} (1 - e^{-\lambda_z t_1})}{\frac{1}{\lambda_x} (1 - e^{-\lambda_x t_1})} \frac{e^{-\lambda_z t_2}}{e^{-\lambda_x t_2}} \right] \quad (12)$$

This equation applies to Y^{89}/Y^{91} where Y^{89} is a stable end product of Sr^{89} and Y^{91} is a radioactive isotope with a 57 day half-life.

APPENDIX B

Corrections for Ce contamination

The masses ^{140}Ce and ^{142}Ce , as measured in Table XI, are made up of both fission Ce and stable Ce contamination

$$\text{i.e. } \frac{\text{Ce}^{140}/\text{Ce}^{142}}{\text{Ce}^{140}/\text{Ce}^{142}} = \frac{\text{F}^{140} + \text{C}^{140}}{\text{F}^{142} + \text{C}^{142}} \quad (13)$$

where $\text{Ce}^{140}/\text{Ce}^{142}$ = observed yields after correction for presence of Nd = 1.37,

F = amount of Ce formed in fission,

and C = amount of Ce contamination.

But $\text{F}^{140}/\text{F}^{142} = 1.00$ (?)

and $\text{C}^{140}/\text{C}^{142} = 7.99$ from natural abundances (46).

Solving equation (13), using these values, gives

$$\text{F}^{142}/\text{C}^{142} = 17.9 \quad (14)$$

$$\text{Also } \frac{\text{F}^{142} + \text{C}^{142}}{\text{F}^{144}} = \frac{\text{Ce}^{142}}{\text{Ce}^{144}} = \frac{1.00}{0.450} \quad (15)$$

Substituting equation (14) in equation (15) and solving gives $\text{F}^{142}/\text{F}^{144} = 2.095$ for Cerium.

This value has been normalized to mass ^{142}Ce in Table XI.

APPENDIX C

Determination of Absolute Fission Yields

The number of atoms of species x, N_x , produced in U^{233} fission is given by the relation

$$N_x = N_{U^{233}} \sigma_{fU^{233}} \phi t f_x \quad (16)$$

where $N_{U^{233}}$ = number of atoms of U^{233} present

$\sigma_{fU^{233}}$ = the fission cross section of U^{233} = 533 barns (37)

ϕ = number of neutrons /cm² /sec. passing through sample

t = length of irradiation

f_x = the fission yield of species x.

Thus
$$f_x = \frac{N_x}{N_{U^{233}} \sigma_{fU^{233}} \phi t} \cdot \frac{1}{\phi t} \quad (17)$$

N_x is obtained by isotope dilution.

Consider the special case of cesium where $N_x = N^{137}$.

Let R_1 = ratio of Cs^{133}/Cs^{137} before isotope dilution.

Let R_2 = ratio of Cs^{133}/Cs^{137} after isotope dilution.

Let the number of atoms of mass 133 present in R_1 be β .

Then the number of atoms of mass 137 present is β/R_1 .

If N^{133} atoms of mass 133 were added during dilution

$$R_2 = \frac{\beta + N^{133}}{\beta/R_1}$$

whence
$$\beta = \frac{R_1}{R_2 - R_1} \cdot N^{133}$$

Then $N^{137} = \beta/R_1 = \frac{N^{133}}{R_2 - R_1}$ is the number of atoms in the

fraction of stock diluted. If $1/n^{\text{th}}$ of stock was diluted the number of atoms of mass 137 produced in the total sample is $\frac{N^{133}}{R_2 - R_1} \cdot n$.

A similar equation may be applied to determine the absolute yield of Nd^{143} .

APPENDIX D

Self-Shielding of the Irradiated Samples

The self-shielding correction is defined as Flux within Material/Flux external to Material. Case, Hoffmann and Flacsck (53) have published tables which are based on the neutron diffusion theory, relating the collision probability, P_c , to the sample dimensions and neutron mean free path in the material. The self-shielding factor is equal to $(1 - P_c)$.

The mean free path of a neutron in a given material is expressed by the relation

$$L = \frac{1}{N\sigma} \quad (13)$$

where L is the mean free path,

N is the number of neutron-absorbing atoms per unit volume,

and σ is the effective neutron absorption cross section of the absorbing atoms.

The thermal neutron absorption cross section of Samples B and C may be calculated from the relative abundance of the U^{236} and U^{235} in the sample and the thermal neutron absorption cross sections of U^{236} and U^{235} . Thus

$$\sigma_a = \left(\frac{1}{15.02} \times 533 \right) + \left(\frac{14.02}{15.02} \times 2.3 \right) = 38.10 \text{ barns}$$

where the ratio $U^{236}/U^{235} = 14.02$ (Table VII)

$$\sigma_{\text{abs}} \text{ for } U^{235} = 533 \text{ barns (37)}$$

$$\text{and } \sigma_{\text{abs}} \text{ for } U^{236} = 2.3 \text{ barns (37).}$$

The effective neutron absorption cross section of the uranium isotope mixture in Samples B and C for a Maxwellian neutron distribution is, therefore,

$$\sigma_{\text{eff}} = 38.10 \times \sqrt{\frac{\pi}{2}} \sqrt{\frac{293}{330}} = 31.76 \text{ barns}$$

assuming a 57°C neutron temperature (10).

Samples B and C contained 0.0761 gm. and 0.0746 gm. uranium respectively and this was packed in cylindrical vials, B having dimensions 0.072 cm. radius and 3.8 cm. length and C having 0.077 cm. radius and 3.8 cm. length. The number of atoms per unit volume of sample is:

$$\text{for Sample B } N = \frac{0.0761 \times 6.02 \times 10^{23}}{238 \times 0.0620} = 3.11 \times 10^{21} \text{ atoms/cc.}$$

$$\text{for Sample C } N = \frac{0.0746 \times 6.02 \times 10^{23}}{238 \times 0.0713} = 2.65 \times 10^{21} \text{ atoms/cc.}$$

Thus the mean free path of a Maxwellian distribution of thermal neutrons in Sample B is 10.1 cm. and for Sample C is 11.9 cm. from equation (13).

Since these samples approximate in shape that of the infinite cylinder, the self-shielding correction may be estimated from Table 4, given by Case, Hoffmann and Placzek (53) in terms of the ratio of sample radius to the mean free path.

$$\text{For Sample B } \frac{\text{Radius}}{\text{mean free path}} = \frac{0.072}{10.1} = 0.007$$

and the self-shielding factor $(1 - P_c) = 0.99$

For Sample C $\frac{\text{Radius}}{\text{Mean free path}} = \frac{0.077}{11.9} = 0.006$

and the self-shielding factor $(1 - P_0) = 0.99$

Because the self-shielding is less than 1% in each case, it has been considered negligible and no allowance has been made for any variation in flux between the cobalt monitors and the uranium samples in calculating the fission yields.